Characterization of the Novel Photosynthetic Protein PPP7 involved in Cyclic Electron Flow around PSI

Dissertation

zur Erlangung des Doktorgrades der Fakultät für Biologie

der Ludwig-Maximilians-Universität München

Vorgelegt von

Giovanni Dal Corso

aus Verona

Italien

München

Dezember 2007

Summary

Photosynthetic organisms are able to convert light energy into chemical energy by the operation of the two photosystems, the cytochrome b_6/f complex and the ATPase. The two photosystems operate in series during linear electron flow to split H_2O and to generate $NADP^+$. During electron transport, a pH gradient is generated across the thylakoid membrane which is used for the generation of ATP. In addition to the linear electron transport mode, ATP can also be produced via cyclic electron flow around photosystem I (CEF). The physiological role of CEF in vascular plants with C_3-type photosynthesis is still not solved. Potential functions of CEF are (i) the dissipation of excessive light energy by increasing non-photochemical quenching (NPQ); (ii) ATP synthesis during steady-state photosynthesis; (iii) the regulation of the stromal oxidation state under stress conditions and under conditions when the Calvin cycle is not available as a sink for NADPH. With exception of the thylakoid NADPH-dehydrogenase complex and the stromal protein PGR5, the components that contribute to CEF are still unknown. Obscure is also the regulation that controls the switch from linear to cyclic flow. We have identified a novel transmembrane protein, named PPP7, which is located in thylakoids of photoautotrophic eukaryotes. Mutants lacking PPP7 exhibit the same phenotype as plants missing PGR5. These mutants show reduced NPQ, decreased P_{700} oxidation and perturbation of ferredoxin-dependent CEF. The work described in this thesis demonstrates that PPP7 and PGR5 interact physically, and that both co-purify with photosystem I. PPP7 does also interact in yeast assays with the cytochrome b_6/f complex, as well as with the stromal proteins ferredoxin (Fd) and ferredoxin-NADPH oxido-reductase (FNR), but PPP7 is not a constitutive component of any of the major photosynthetic complexes. In consequence, the existence of a PPP7/PGR5 complex integrated in the thylakoid membrane and facilitating CEF around PSI in eukaryotes, possibly by shuttling electrons together with ferredoxin and the FNR from photosystem I to the cytochrome b_6/f complex, is proposed. Moreover, CEF is enhanced in the *Arabidopsis psad1* and *psae1* mutants with a defect in photosystem I oxidation in contrast to the cyanobacterial *psae* mutant which exhibits an decreased CEF, pointing to fundamental mechanistic differences in the cyclic electron flow of cyanobacteria and vascular plants. The *Arabidopsis psad1* and *psae1* mutants also show higher contents of ferredoxin and of the PPP7/PGR5 complex, supporting a role of PPP7 and PGR5 in the switch from linear to cyclic electron flow depending on the redox state of the chloroplast.

Zusammenfassung

Photosynthetisch aktive Organismen sind in der Lage mit Hilfe der Photosysteme, des Cytochrom b_6/f-Komplexes und der ATPase Lichtenergie in chemische Energie umzuwandeln. Wenn die beiden Photosysteme während des linearen Elektronentransports in Serie arbeiten wird Wasser gespalten und NADPH erzeugt. Der durch den Elektronentransport über die Thylakoidmembran aufgebaute Protonengradient dient schließlich der Synthese von ATP. Neben dem linearen Elektronentransport trägt auch der zyklische Elektronenfluß um das Photosystem I zur Produktion von ATP bei. Die physiologische Funktion des zyklischen Elektronentransports bei Gefäßpflanzen mit C3-Photosynthese ist jedoch noch immer nicht eindeutig geklärt. Potentielle Funktionen des zyklischen Elektronentransportes könnten sein: (i) die Ableitung von überschüssiger Lichtenergie durch Erhöhung des nicht photochemischen Quencheffektes (NPQ); (ii) die ATP Synthese während der Photosynthesereaktion im stationären Zustand; oder (iii) die Regulation des stromalen Redoxzustandes unter Stressbedingungen und Bedingungen, unter denen der Calvin-Zyklus nicht als Akzeptor von NADPH zur Verfügung steht. Mit Ausnahme des in der Thylakoidmembran lokalisierten NADPH-Dehydrogenase Komplexes und des stromalen Proteins PGR5 sind bisher keine weiteren Komponenten bekannt, die zum zyklischen Elektronentransport beitragen. Unklarheit herrscht auch über die Mechanismen, die ein Umschalten von linearem zu zyklischem Elektronentransport kontrollieren. In dieser Arbeit wird die Identifizierung eines Transmembranproteins mit der Bezeichnung PPP7 beschrieben, welches in der Thylakoidmembran von photoautotrophen Eukaryoten lokalisiert ist. Mutanten, denen PPP7 fehlt, zeigen den gleichen Phänotyp wie Pflanzen, die kein PGR5 exprimieren. Beide Mutanten weisen reduzierten NPQ, erniedrigte Oxidation von P700 als auch eine Störung des Ferredoxin-abhängigen zyklischen Elektronentransport auf. Die Arbeiten, die in dieser Dissertation beschrieben werden, zeigen, dass PPP7 und PGR5 direkt miteinander interagieren und dass beide mit Photosystem I aufgereinigt werden können. Das PPP7 Protein interagiert im Hefesystem auch mit dem Cytochrom b_6/f-Komplex und mit den stromalen Proteinen Ferredoxin und Ferredoxin-NADPH-Oxido-Reduktase (FNR), ist jedoch kein konstitutiver Bestandteil der Photosysteme oder von Cytochrom b_6/f oder der ATPase. Wir postulieren daher das Vorhandensein eines in die Thylakoidmembran integrierten Komplexes aus PPP7 und PGR5, der den zyklischen Elektronenfluß um PSI bei Eukaryoten unterstützt, indem er mit Ferredoxin und FNR interagiert und somit möglicherweise als Elektronentransporter zwischen PSI und dem Cytochrom b_6/f-Komplex fungiert. Zudem ist bei den *Arabidopsis* Mutanten *psad1* und *psae1* mit gestörter Oxidation von Photosystem I ein verstärkter zyklischer Elektronentransport messbar, ganz im Gegensatz zu der cyanobakteriellen *psae* Mutante mit erniedrigtem zyklischen Elektronentransport; dies impliziert grundlegende Unterschiede zwischen Cyanobakterien und Pflanzen beim zyklischen Elektronentransport. Die *psae1* und *psad1* Mutanten bei *Arabidopsis* haben zudem einen erhöhten Gehalt an Ferredoxin und an PPP7-PGR5, was auf eine Beteiligung von PPP7 und PGR5 am Umschalten von linearem auf zyklischen Elektronentransport in Abhängigkeit vom Redox-Zustand des Chloroplasten hinweist.

Contents

Abbreviations

°C	Degree Celsius
35SCaMV	35S promoter of the Cauliflower Mosaic virus
ATP	Adenosine triphosphate
BN	Blue native
cDNA	Complementary deoxyribonucleic acid
CEF	Cyclic electron flow
Chl	Chlorophyll
cyt b_6/f	Cytochrome b_6/f complex
Da	Dalton
DNA	Deoxyribonucleic acid
ETR	Electron transport rate
Fd	Ferredoxin
FNR	Ferredoxin NADP oxido-reductase
g	Gram
h	Hour
HPLC	High performance liquid chromatography
L	Liter
LB	Left border
LEF	Linear electron flow
LHC	Light-harvesting complex
Lu	Lutein
m	Meter
M	Molarity
min	Minute
mol	Mole
$NADP^+/H$	Nicotinamide adenine dinucleotide phosphate
NDH	NADPH deydrogenase complex
	or NAD(P)H-plastoquinone-oxidoreductase complex

_____

NPQ	Non-photochemical quenching
Nx	Neoxanthin
OEC	Oxygen evolving complex
P_{700}	PSI reaction centre
PAGE	Polyacrylamide gel electrophoresis
PAM	Pulse amplitude modulation
PCR	Polymerase chain reaction
PFD	Photon flux density
PGR5	Proton gradient regulation 5
PPP7	Putative photosynthetic protein 7
PQ	Plastoquinone
PS	Photosystem
qP	Photochemical quenching
qE	ΔpH-dependent NPQ
RB	Right border
RFP	Red fluorescent protein
RNA	Ribonucleic acid
ROS	Reactive oxygen species
RT-PCR	Reverse transcriptase-polymerase chain reaction
s	Second
SD	Standard deviation
SDS	Sodium dodecyl sulphate
T-DNA	Transfer-DNA
$^v/_v$	Volume per volume
VAZ	Xanthophyll cycle pigments
$^w/_v$	Weight per volume
WT	Wild-type
β-Car	β-carotene
β-DM	n-dodecyl β-D-maltoside
Φ_{II}	Effective quantum yield of photosystem II

1. Introduction

1.1 <u>Photosynthesis</u>

Life on Earth ultimately depends on the energy coming from the sun and photosynthesis is the only known biological process that can utilise this energy and convert it into chemical energy and organic substances. Photosynthetic organisms (from photosynthetic prokaryotes to flowering plants) use solar energy to synthesize carbon compounds from carbon dioxide and water. In photosynthetic organisms, the photosynthetic reactions take place in a specialized organelle derived from ancient photosynthetic prokaryotes, the chloroplast. In the chloroplast, light energy is converted into chemical energy by a number of different complexes working together, all embedded in the thylakoid membranes. As described schematically in **Figure 1.1** light energy drives the electron transfer from photosystem II (PSII) via photosystem I (PSI) to the final electron acceptor $NADP^+$. Coupled with the linear electron transport, protons (H^+) are transported into the thylakoid lumen by the Q-cycle at the cytochrome b_6/f complex. The activity of the oxygen evolving complex (OEC) located at the PSII contributes to increase the H^+ amount in the lumen. These protons then diffuse to the ATP synthase, where their diffusion down the electrochemical potential gradient is used to synthesize ATP in the stroma. ATP and NADPH are subsequently used in the stroma as an energy source and reducing power for the biosynthesis of organic compounds like synthesis of amino acids, nucleotides, fatty acids and lipids, vitamins, hormones and assimilation of sulphur and nitrogen.
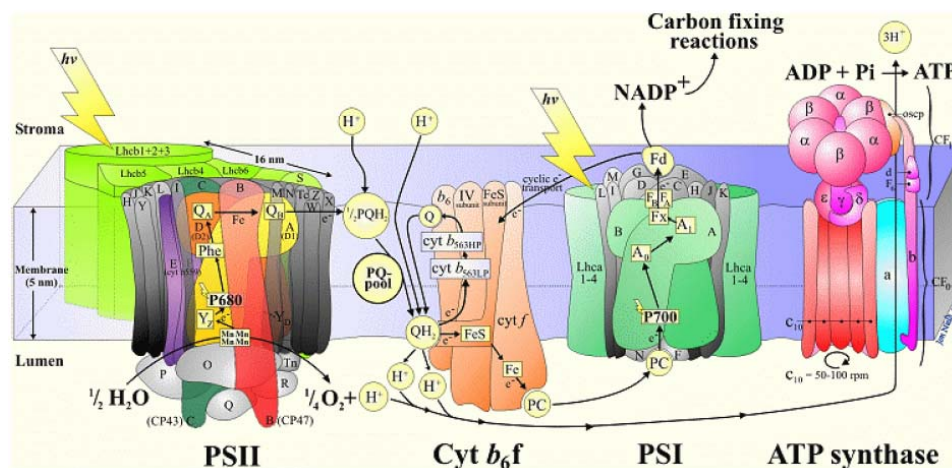
Fig 1.1. Scheme of electron transport chain in thylakoids. From Jon Nield, Imperial College London, 2000.

_____

The electron transfer from H_2O to $NADP^+$ through the PSII - cyt b_6/f - PSI complexes is termed linear electron flow (LEF). Already in 1955 Arnon *et al.* described a pathway of cyclic electron flow (CEF) around PSI responsible for the generation of a ΔpH across the thylakoid membrane without accumulation of NADPH. In this pathway, electrons of the PSI go back to the cytochrome b_6/f complex and than again to PSI via plastocyanin.

1.2 <u>Novel putative photosynthetic proteins</u>

Over the past few decades, knowledge about the organization and function of all the major super-complexes forming the photosynthetic machinery has been accumulated, but many of the minor components or proteins embedded or simply associated to the thylakoid membrane have not been identified yet. A powerful tool to attribute a function to an unknown gene is the so called "transcriptomics" approach in which the expression patterns of genes are compared. This approach is based on the assumption that genes with correlated expression patterns are most likely to have related functions. Those groups of genes are known as regulons (cluster of genes of co-expressed profiles). In 2005, the definition and characterization of regulons of a number of nuclear genes of *Arabidopsis thaliana* have been reported (Biehl *et al.*, 2005). The mRNA expression of 3292 nuclear genes, most of them coding for chloroplast proteins (Richly *et al.*, 2003) was determined under a total of 101 different environmental and genetic conditions. This analysis showed that many photosynthetic genes and genes for proteins of the plastid ribosome can be grouped together on the basis of their very similar expression pattern. In other words, the co-regulation of the expression of genes for photosynthetic proteins and of genes for plastid ribosome can be interpreted as a mechanism to ensure that the subunits of those multi-protein complexes are synthesized in matching amounts (Biehl *et al.*, 2005). One of the unknown proteins being co-regulated with photosynthetic genes is the subject of this thesis and has been named PPP7 (Putative Photosynthetic Protein 7).

## 1.3 <u>Cyclic electron flow: from PSI to PSI</u>

Although the *in vivo* occurrence of CEF has been subject of controversy, it is well established in isolated systems and *in vitro* models (Johnson, 2005). Most of the still unsolved questions about CEF concern the components that play a role as donors, sinks and

carriers of electrons. Since it was observed that CEF enhances the formation of a ΔpH (Arnon, 1965), it was postulated that there must exist an enzyme that transfers electrons to the plastoquinone pool which then would supply the cytochrome b_6/f complex with electrons, assuming that the plastoquinone pool is the ultimate electron acceptor prior to cytochrome b_6/f.

Once the electrons are transferred to the oxidised plastoquinone pool, they most probably follow the normal way through cytochrome f and palstocyanin to P_{700} of PSI (Johnson, 2005). Regarding the route that electrons follow up-stream of PQ, it has been reported that ferredoxin is required as a cofactor for cyclic photophosphorylation (Tagawa *et al.*, 1963) and that this pathway is sensitive to antimycin A, an inhibitor known to interact with the Q_i binding pocket on the stromal side of the cytochrome b_6/f complex. However, Moss and Bendall (1984) showed that HQNO (2-(n-heptyl)-4-hydroxyquinoline N-oxide, an inhibitor of cytochrome b) does not affect CEF, leading to the idea that a distinct enzyme should be involved. Unfortunately, until now there exists no biochemical evidence for the presence of this putative ferredoxin-plastoquinone oxidoreductase enzyme (FQR). One of the possible pathways that electrons could follow from the acceptor side of PSI to the PQ pool is known as the "ferredoxin dependent-antimycin sensitive" pathway. In 2001, Zhang *et al*. could show that ferredoxin-NADPH-oxidoreductase (FNR) binds tightly to the cytochrome b_6/f complex suggesting the formation of a complex together with ferredoxin, which would then create a bridge for the electron transfer to the PQ pool.

Evidences also exist for another pathway that is insensitive to antimycin A. It involves the NDH enzyme (NADPH dehydrogenase) located in the thylakoid membrane. This enzyme is homologous to the NADH dehydrogenase complex (complex I) of mitochondria. The first evidences that the NDH enzyme is involved in CEF have been found in the cyanobacterium *Synechocystis* (PCC6803). It was found that a mutant defective in ndhB has an impaired CEF around PSI (Mi *et al.*, 1995). Also the plastome of higher plants contains at least 11 genes that code for subunits of the NDH complex (reviewed in Shikanai, 2007). The plastidic NDH has a higher similarity to the cyanobacterial complex than to the ones of the mitochondrial complex I within the same species, suggesting an evolutionary and functional similarity for the NDH complexes of cyanobacteria and chloroplasts. By using chloroplast transformation techniques, it has been shown that mutant

plants defective in the NDH complex had a slightly reduced CEF. This suggests a role of NDH in the electron transport from the stromal electron pool to PQ (Burrows *et al.*, 1998, Kofer *et al.*, 1998, Shikanai *et al.*, 1998). Many authors criticise that the detectable concentration of the NDH enzyme is too low to sustain a significant rate of CEF (<1% per photosynthetic electron chain, Sazanov *et al.*, 1998, Joet *et al.*, 2002), whereas others argue that the rapidly induced cyclic flow is not compatible with the rather low activity of this enzyme (Breyton *et al.*, 2006). Answering the questions about mechanisms and pathways followed by electrons to cycle around PSI is one of the last major tasks to be solved in this research field of photosynthesis.
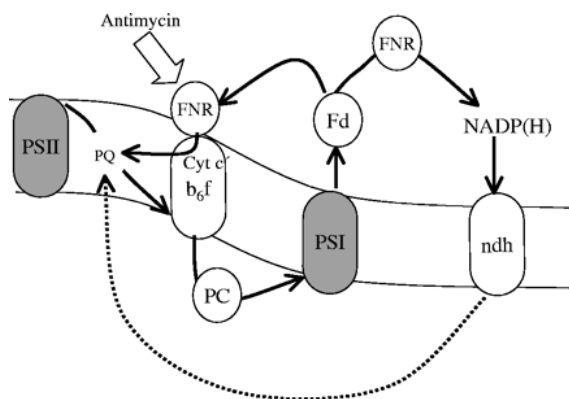
Fig 1.2. Possible routes followed by electrons from the PSI acceptor side to the PSI donor side. (Johnson, 2005).

1.4 Measuring cyclic electron flow

One of the main problems studying cyclic electron flow is the fact that the electron carriers of the cyclic pathway are also involved in linear electron transport (i.e. cytochrome b_6/f complex, PSI, Fd and $NADP^+$). For this reason, all developed techniques, both *in vitro* and *in vivo*, try to determine the relative contribution of cyclic flow to the total electron flux through the shared components. Some of the most commonly used techniques are briefly explained in the following sections.

1. **Chlorophyll fluorescence analysis.** Using a PAM fluorometer, the electron flow can be monitored *in vivo* by a change in chlorophyll fluorescence. In particular, the electron flow from NADPH to the intersystem chain can be roughly estimated by transient increase in chlorophyll fluorescence after a period of illumination with actinic light

(Schreiber *et al.*, 1986). The fact that far-red light, which activates predominantly PSI photochemistry, is able to quench this increase in fluorescence demonstrates that NADPH transfers electrons to the plastoquinone pool (Shikanai *et al.*, 1998).

2. **Fd-dependent PQ reduction assay**. The reduction of plastoquinone can be monitored as an increase in chlorophyll fluorescence emitted after the exposure to light of a very low intensity (1 $\mu Em^{-2}s^{-1}$). At such low light intensities, the fluorescence reflects the reduction of plastoquinone by cyclic electron transport from ferredoxin, not by PSII photochemistry (Munekage *et al.*, 2002). This system can be applied to *in vitro* ruptured chloroplasts, using exogenous ferredoxin and NADPH as an electron source.

3. **Photoacoustic techniques.** The photoacoustic method is based on the ability of modulated light to produce a sound upon absorption (Malkin and Canaani, 1994). It was developed to quantitatively evaluate the storage of photosynthetic energy by cyclic electron flow in intact leaves or algae, as well as in isolated thylakoids (Herbert *et al.*, 1990). In brief, photoacoustic signals are used to quantify the conversion of absorbed light to heat in a sample. If no photochemistry is performed by the sample, the conversion is 100%. However, if some of the light energy is stored as photochemistry products, e.g. in leaf or algal sample performing photosynthesis, it is not available for conversion to heat anymore and changes the thermal photoacoustic signal in a way that can be quantified. Using far red light as an exciting source, only PSI is functioning and the photoacoustic signal reflects the cyclic electron flow (Joet *et al.*, 2002). Using this technique, energy storage due to CEF could be observed in cyanobacteria, algae and C_4 plants, and to a lesser extent also in C_3 plants (Herbert *et al.*, 1990; Joet *et al.*, 2002).

4. **P_{700} re-reduction measurements**. The illumination of a leaf with far red light ($\lambda >$ 700nm) excites only PSI and not (or only partially) PSII. Under those conditions, the rate of electron flow from PSII to PSI is negligible (Joliot and Joliot, 2005). After a period of illumination, the light is switch off and the P_{700} redox state can be measured as a change in absorbance at 700 nm or at the near infrared range (810-860 nm) (Johnson, 2005). The reduction rate of P_{700} immediately after the cessation of light is thought to be proportional to the rate of electron flow occurring in light through PSI. A general accepted approach is to assume that the proportion of P_{700} in the reduced state is a value for the quantum efficiency of PSI (Harbinson and Woodward, 1987). The re-

reduction kinetics of P_{700} in the dark accelerates when electrons coming from the stroma are donated to PSI. This fast reduction has been observed in algae, cyanobacteria and C_4 plants. This reduction takes place also in C_3 plants with a reduced rate, probably due to a lower NDH activity (Munekage and Shikanai, 2005).

5. **Use of inhibitors**. Methylviologen is well known to accept electrons from PSI (Ivanov *et al.*, 2007) forcing the photosynthetic chain to operate only in linear electron flow (Joliot and Joliot, 2005). The involvement of PQ and the cytochrome b_6/f complex in CEF around PSI was shown by studies using inhibitors like DCMU (3-(3,4-dichlorophenyl)-1,1-dimethiylurea) which binds to the Q_B site of PSII or HQNO (2-heptyl-4-hydroxyquinolines) which binds to the cytochrome b_6/f complex (Munekage and Shikanai, 2005). In these studies, DCMU was shown not to inhibit cyclic electron transport (Bendall and Manasse, 1995). Finally, a vexing question is still open about the activity of antimycin A, an inhibitor supposed to bind the Q_i binding site of the cytochrome b_6/f complex interrupting the Fd-dependent CEF pathway (Okegawa *et al.*, 2005).

1.5 <u>Models of cyclic electron flow</u>

CEF and LEF share a number of common electron carriers, from plastoquinone to ferredoxin (Breyton *et al.*, 2006). In the following, different models on the organization of the "cyclic" machinery are discussed:

1. **The diffusion model**. It is generally accepted that the different multi-protein complexes are heterogeneously distributed in the thylakoid membrane; in particular, PSII is mostly located in the grana stacks while PSI is more abundant in the non-compressed stromal lamellae, in the margin and end membranes of the grana stacks (Allen and Forsberg, 2001). The cytochrome b_6/f complex, on the other hand, is homogenously distributed over the thylakoid membranes (Albertsson 2001). In this model, only the cytochrome b_6/f complexes located in the non-appressed membranes would receive electrons from PSI resulting in CEF, while in the grana stacks the plastoquinone pool is exclusively reduced by PSII (Albertsson 2001; Bukhov and Carpentier, 2004).

_____

2. **The super-complex model.** Already in 1967 Boardman and Anderson found super-complexes of PSI and cytochrome b_6/f in *Chlamydomonas* and vascular plants. FNR is also known to associate with cytochrome b_6/f (Zhang *et al*., 2001). These findings led to the postulation of a tightly associated complex of FNR, PSI and cytochrome b_6/f which would take over electrons from ferredoxin, fuelling the cyclic pathways (Joliot and Joliot, 2002). Recent biochemical approaches aimed to confirm an eventual FNR-PSI-cytochrome b_6/f super-complex failed, however, to prove its existence (Breyton *et al*., 2006).

3. **The FNR model.** FNR has been found to be associated with both PSI (Scheller *et al*., 2001) and the cytochrome b_6/f complex (Zhang *et al*., 2001). Joliot and Joliot (2005) proposed that PSI-FNR complexes transfer electrons from Fd to NADP$^+$, via linear electron flow, while the population of FNR associated with the cytochrome b_6/f complex is responsible for the cyclic electron pathway from ferredoxin (reduced by those PSI not associated with the FNR) to plastoquinone (**Figure 1.3**).
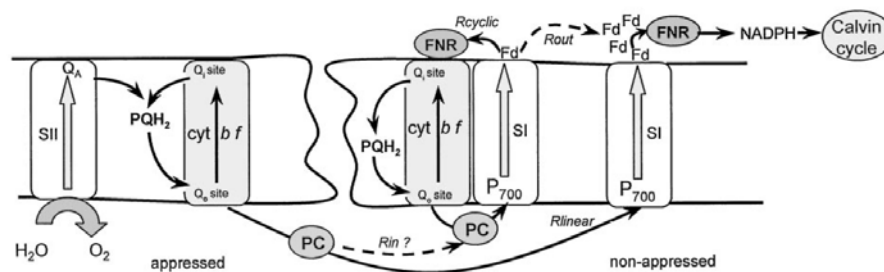
Fig 1.3. Possible routes followed by electrons from the PSI acceptor side to the PSI donor side. (SII: PSII and SI: PSI), from Joliot and Joliot (2002).

1.6 The role of cyclic electron flow in C$_3$ plants

There are two major conditions under which CEF plays a significant role in photosynthesis:

1. **during the transition dark-to-light**. During this brief period of time (within minutes), the majority of the enzymes involved in the Calvin cycle have to be newly synthesized or activated, most importantly Rubisco, fructose-1,6-bisphostphate phosphatase, sedoheptulose-1,7-bisphospate phosphatase, ribulose-5-phosphate kinase and NADP-glyceraldehyde-3-phosphate dehydrogenase. Moreover, the main intermediate of the

Calvin cycle (ribulose-1,5-bisphosphate) has to be synthesized. As an example, the activation of Rubisco requires ATP and an increase in the stromal pH (Campbell and Ogren, 1992)). The activation of the other enzymes listed before requires reduced ferredoxin, which then can activate the thioredoxin regulatory system. Reduced ferredoxin, increase in stromal pH and ATP production are all factors influenced by cyclic electron flow (Munekage *et al.*, 2002). Indeed, during the first minutes of illumination of dark adapted leaves, high rate of CEF can be measured (Laisk *et al.*, 2005; Joliot and Joliot, 2002).

2. **<u>during steady state of photosynthesis</u>**. In contrast to LEF, CEF can generate a ΔpH without accumulation of NADPH. It can also modify the ratio between proton translocation and electron transport and eventually the ratio of ATP/NADPH production (Munekage and Shikanai, 2005). Owing to only linear electron flow, the ATP/NADPH ratio is 1.29. On the other hand, the requirement for the Calvin Cycle is 1.5 to 1.66 depending on the amount of photorespiration (Osmond, 1981) that corresponds to roughly 20% more of ATP. It has been proposed that CEF could provide this ATP portion needed for the activity of the Calvin cycle during steady state photosynthesis. This could explain the decreased fitness of mutants defective in cyclic electron flow (see below in this section).

To prevent photoinhibition caused by excessive absorption of light energy, plants developed different mechanisms. The most effective is thermal dissipation, which is induced by the generated ΔpH across the thylakoid membrane (Müller *et al.*, 2001). In this respect, CEF may regulate the induction of thermal dissipation modifying the generation of the ΔpH (Heber and Walker, 1992). Supporting this hypothesis, in 1999 the *Arabidopsis thaliana* mutant *pgr5* has been discovered as a high chlorophyll fluorescence mutant impaired in CEF (Shikanai *el al.*, 1999).

The finding that in ruptured chloroplasts, exogenous electron donors like ferredoxin or NADPH, trigger cyclic electron transport independently from PSI photochemistry (Mills *et al.*, 1979), suggests that CEF is promoted by reducing power within the chloroplast. In other words, CEF might be regulated by the redox state of the chloroplast (Bukhov *et al.*, 2002; Nandha *et al.*, 2007).

Under stress conditions, such as high light, the partial pressure of available CO_2 for the

Rubisco activity is reduced, while the NPQ increases. In tobacco, for example, the activity of CEF relative to that of LEF is enhanced under stress conditions, contributing to the induction of NPQ by generating a ΔpH across the membrane (Miyake *et al.*, 2005). Indeed, tobacco mutants defective in the NDH complex are more sensitive to high light stresses (Endo *et al.*, 1999). As already confirmed by *in vitro* experiments (Endo *et al.*, 1998), reduced forms of Fd and NADPH lead to the activation of CEF pathways.

Other critical conditions for a plant's performance are drought and high temperatures, similar conditions under which the stomatal closure and a higher transpiration rate create a reduced availability of CO_2. Furthermore, high temperatures decrease the Rubisco activity leading to an over-reduction of the stromal environment (Crafts-Brandner and Salvucci, 2000). Under such conditions, CEF is activated, generating a proton gradient that induces NPQ which is involved in dissipating excessive energy (Golding and Johnson, 2004).

CEF could be considered as a "safety valve" in which electrons are (re)cycled around PSI and thus, oxygen reduction and consequently reactive oxygen species (ROS) production are minimized. According to this hypothesis, PSI of the *pgr5* mutant is highly sensitive to photoinhibition even at low light intensities (Munekage *et al.*, 2002). This cannot be attributed to a lack of NPQ, since this effect does not occur in mutants with blocked qE (e.g. *npq4*, Munekage and Shikanai, 2005).

Recently *Arabidopsis* mutant, *pgr5 crr*, has been generated defective in both the Fd-dependent (*pgr5* mutation) as well as in the NDH dependent (*crr* mutation) pathways. The mutant plants show a dramatic reduction in photosynthetic growth (Munekage *et al.*, 2004), suggesting that cyclic electron transport around PSI is required for efficient photosynthesis and autotrophic growth. However, the lack of a generally accepted technique to measure CEF *in vivo* and the still limited knowledge of the molecular mechanisms that drive CEF result in contrary hypotheses about the role of CEF around PSI in C_3 plants especially under environmental growth conditions.

1.7 <u>The role of cyclic electron flow in C_4 plants</u>

In the bundle-sheath cells of C_4 plants, cyclic electron flow is thought to play an important role. It is well known that C_4 plants can generate a high CO_2 concentration by minimizing

the dissipating oxygenase activity of Rubisco, but such alternative C fixation system costs them about two additional molecules of ATP to fix one molecule of CO_2 compared with C_3 plants. Moreover, in the bundle-sheath cells of C_4 plants, the reduced packing of the thylakoids in grana stacks gives a higher PSI/PSII ratio than in C_3 plants (Takabayashi *et al.*, 2005). This thylakoid organization determines that in the bundle-sheath cells, PSII amounts and activity are highly reduced compared to the mesophyll cells (Romanowska *et al.*, 2006). This strongly suggests that no significant linear electron transport occurs in bundle-sheath thylakoids (Bassi *et al.*, 1995). An enhancement of CEF would provide the extra ATP that could be used for CO_2 fixation reactions. Recently it has been found that in the C_4 plants belonging to the NADP-ME family (e.g. *Sorghum bicolor* and *Zea mays*) the amount of the NDH complex is significantly higher in bundle-sheath cells in comparison to the mesophyll's and at least ten times higher than in the thylakoids of the C_3 plant tobacco. Interestingly, the homologue of the *Arabidopsis* PGR5 protein accumulates rather uniformly in mesophyll and bundle-sheath cells and the amounts are comparable with those of tobacco or *Arabidopsis*. These findings indicate that CEF plays a role in the production of additional ATP in the C_4 metabolism (Takabayashi *et al.*, 2005).

1.8 The role of cyclic electron flow in cyanobacteria and unicellular eukaryotes

NDH activity has been found in both cyanobacteria (Mi *et al.*, 1992, 1994) and algae (Seidel-Guyenot *et al.*, 1996). So far eleven genes coding for the subunits of this complex have been identified in the genomes of both types of organisms.

a) **Cyanobacteria**. The first aspect that has to be considered is that the diazotrophic cyanobacteria need to separate nitrogen fixation from photosynthesis, since that the nitrogenase enzyme is highly sensitive to molecular oxygen (Berman-Frank *et al.*, 2003). To prevent inhibition, the nitrogenase complex is confined in specialized cells called heterocysts. Since heterocysts lack O_2-producing photosystem II (Wolk *et al.*, 1994) they generate ATP through CEF around photosystem I (Ernst *et al.*, 1983). Moreover, *Synechococcus* and *Synechocystis* mutants lacking or being defective in the NDH complex, show impaired inorganic carbon assimilation (Bukhov and Carpentier, 2004) and show impaired CEF around PSI. Additionally, in *Synechocystis* the homologue of PGR5

_____

(ssr2016) has been reported (Yeremenko *et al.*, 2005). As in flowering plants, this protein is thought to play a role in an antimycin-A sensitive pathway of CEF.

Thus, it has been suggested that the ssr2016 pathway is not a major contributor to CEF but has a regulatory function, sensing the redox balance of the cytoplasm. In fact it is strongly induced by high light intensities or salt stress (Allakhverdiev *et al.*, 2002; Kanesaki *et al.*, 2002). Under such circumstances, the most of the required ATP, needed for repair and stress-activated mechanisms, could be supplied by CEF (Thomas *et al.*, 2001). It has been found that subunits of PSI (for instance PsaE) are involved in CEF (Zhao *et al.*, 1993; Yu *et al.*, 1993) and the *ndh/psaE* double knock out does not show any CEF around PSI (Yu *et al.*, 1993). Besides the NDH- and the PGR5-dependent pathways, there is evidence for the existence of further pathways of PSI-mediated CEF, differentially induced by environmental conditions (Cooley *et al.*, 2000; Matthijs *et al.*, 2002).

b) **Algae**. Unlike in vascular plants, in unicellular green algae (e.g. *Chlamydomonas*) a large fraction of the LHCII (about 80%) migrates to PSI under light conditions favouring PSII (Allen, 1992). This phenomenon, known as state transition, causes a switch between linear and cyclic electron flow. The finding that the injection of electrons in the cytochrome b_6/f complex is insensitive to the addition of PSII inhibitors during state 2 confirmed that electrons re-cycle (Finazzi *et al.*, 1999, Finazzi and Forti, 2004). The plastome of *Chlamydomonas* does not code for the 11 genes of the subunits of the NDH complex (Shikanai, 2006), but its genome codes for a homologue of the *Arabidopsis* PGR5 protein, supporting an involvement of this pathway in this switch between linear and cyclic flow, even though the precise role and contribution of it is still not clear.

1.9 Cyclic electron flow: a genetic approach

As mentioned before, it is generally accepted that in flowering plants exist two partially redundant routes that electrons can follow to cycle around PSI. One is via the thylakoid NDH complex (Shikanai *et al.*, 1998), and the other is probably involving ferredoxin and the protein PGR5 (Munekage *et al.*, 2002).

The NADPH dehydrogenase complex

The thylakoidal NDH complex is a multi-protein complex whose structure has not been elucidated yet. The plastome contains 11 genes (*ndhA* to *ndhK*) that are homologues to the

_____

bacterial *ndh* genes. Further three subunits are present in bacteria, but not encoded by the plastome of higher plants. These missing subunits are involved in the formation of the docking site for NAD(P)H and its oxidation (Rumeau *et al.*, 2005). The nature of the "electron input subunit" of the plastidial NDH is still unclear. It has been proposed that FNR could interact with the NDH complex supplying electrons derived from NADPH reduction. Recently it has been suggested that also reduced ferredoxin could represent an electron source, in which case the FNR enzyme would play a significant role as an electron shuttle (Shikanai, 2007). Alternatively, in plastidial NDH a new and still unidentified electron input module could be present even if the attempts to purify the plastidial complex did not reveal any missing subunits involved in electron input (Rumeau *et al.*, 2005). In the 1990s by means of plastome transformation techniques (Svab and Maliga, 1993), almost all of the 11 plastidial *ndh* genes were inactivated. The different knockout lines displayed an alteration in electron transport in chloroplasts and an inhibited reduction of the plastoquinone pool. In particular, lines with an altered or missing thylakoid NDH complex showed reduced levels of a transient increase in fluorescence (see **Figure 1.4**) which could be attributed to the electron transfer from the reduced stromal electron pool to the PQ pool (Burrows *et al.*, 1998; Kofer *et al.*, 1998; Shikanai *et al.*, 1998). Recently, the identification of three novel nuclear-encoded subunits for the plastidic NDH (NDH-M, -N and -O) has been reported. The corresponding mutants show a phenotype comparable to the other *ndh*-mutants (Rumeau *et al.*, 2005).
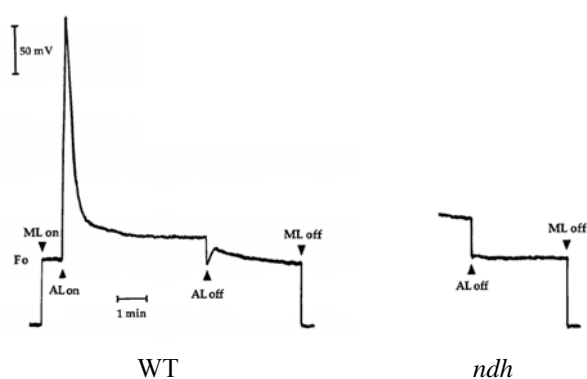
Fig 1.4. Typical fluorescence phenotype of a mutant without functional plastidial NDH: the transient increase of the fluorescence after switching off the light (AL off) is reduced. (Adapted from Kofer *et al.* (1998); ML: measuring light, AL: actinic light; Fo: base fluorescence).

_____

The antimycin A sensitive pathway

Given that cyclic electron flow is involved in ΔpH generation, it should play a role in the induction of non-photochemical quenching (Heber and Walker, 1992). In case a mutant is defective in CEF it should be identifiable due to its defective NPQ phenotype. As already discussed, the amount of NDH is too low for a significant contribution of this complex to an increase in NPQ (Shikanai *et al.*, 1998). Thus, any mutant defective in CEF with a marked NPQ reduction should be defective in a NDH-independent pathway. Using chlorophyll fluorescence imaging, the *Arabidopsis* mutant *pgr5* (***p**roton **g**radient **r**egulation*) has been identified based on its NPQ phenotype (Shikanai *et al.*, 1999). In *pgr5*, the ratio of P_{700} oxidised to P_{700} reduced is lowered at high light intensities, in contrast to the WT. The WT phenotype can be restored by infiltration with methylviologen (electron acceptor of PSI) indicating that electron transport is limited at the acceptor side of PSI (Munekage and Shikanai, 2005). LEF was not affected in isolated thylakoids of *pgr5*, while it is reduced *in vivo* (Munekage *et al.*, 2005). The ferredoxin-dependent plastoquinone reduction was also assayed in ruptured chloroplasts of *pgr5*, and it has been shown that this *pgr5* phenotype can be "simulated" in WT chloroplasts by antimycin A treatment. *PGR5* encodes for a 10 kDa protein associated with the thylakoid membrane (Munekage *et al.*, 2002). PGR5 does not contain any known metal-binding or transmembrane motif and is stable in mutant backgrounds lacking PSII, PSI, the cytochrome b_6/f complex or ATPase, suggesting that PGR5 is not a constituent of any of these major complexes (Munekage and Shikanai, 2005). The exact localisation of PGR5 in the thylakoid membrane is still not clear and its role in CEF is still under debate.

A knock-out mutant entirely lacking CEF

Recently, the group of Shikanai created a series of double mutants by crossing mutants missing or defective in the NDH complex (*crr* mutants) and *pgr5* (Munekage *et al.,* 2004). The double mutants showed a retarded development and growth, pale green colour and defects in linear electron flow (**Figure 1.5**).

_____
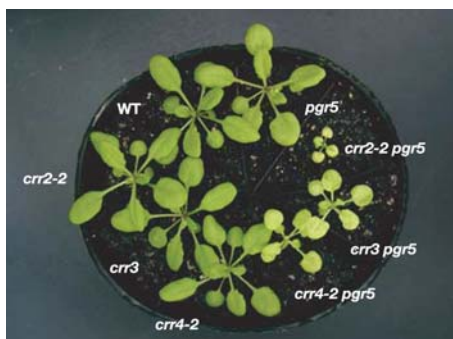
Fig 1.5. Growth phenotypes of WT, *crr2-2*, *crr3*, *crr4-2* and *pgr5* single mutants as well as the *crr4-2pgr5*, *crr3pgr5* and *crr2-2pgr5* double mutants. From Munekage *et al.* (2004).

The plastoquinone reduction activity in ruptured chloroplasts of the double mutants is completely abolished (see **Figure 1.6**). The treatment of ruptured chloroplast of the *crr2-2* mutants with antimycin A mimics the effect of the double mutation. On the other hand, the inhibitor does not have any effects on *pgr5* mutant. This result clearly shows that CRR2 and PGR5 are involved in two different pathways of CEF and that the antimycin A is affecting only the "PGR5 pathway" (Munekage *et al.*, 2004).
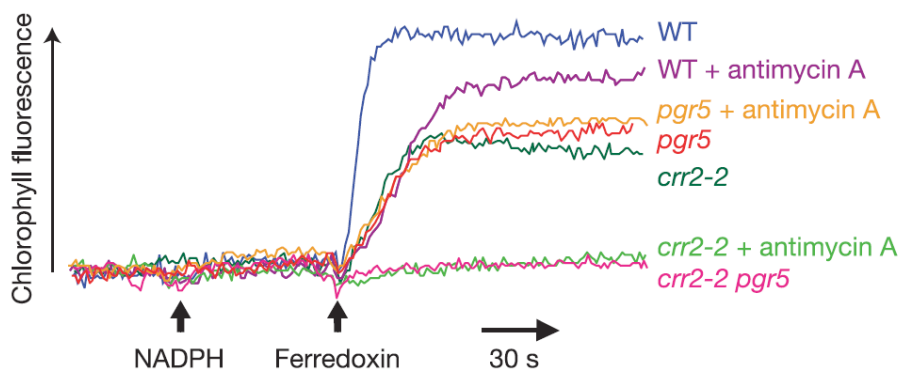
Fig 1.6. Electron transfer to plastoquinone in ruptured chloroplasts measured as an increase in chlorophyll fluorescence after the addition of NADPH and ferredoxin under illumination with weak actinic light. From Munekage *et al.* (2004).

These findings, together with the fact that mutants lacking the entire CEF apparatus (*crr pgr5*) are defective in photoautotrophic growth, show that CEF is important for plant fitness and plays a crucial role in preventing stroma over-reduction (Munekage *et al.*,

_____

2004). In WT plants, this is achieved by adjusting the concentration of ATP and hence keeping a correct ratio ATP/NADPH.

1.10 <u>Aim of the thesis</u>

In this thesis a new **p**utative **p**hotosynthetic **p**rotein (PPP7) identified on the basis of its transcriptional co-regulation with known photosynthetic genes was functionally characterized. The first aim of the thesis was to clarify whether PPP7 is truly a new thylakoid protein. The second aim was to characterize the function of the PPP7 protein by identifying lines which lack the PPP7 protein in a reverse genetics approach and by characterizing those loss-of-function lines on the physiological level. When it became clear in the course of the thesis that PPP7 is involved in cyclic electron flow, an in-depth biochemical and genetic characterization of the role of PPP7 in cyclic electron flow was initiated, including the identification of its interaction partners. In a final step the entire set of data was combined to develop a new model on how cyclic electron flow functions in flowering plants.

_____

2. Materials and Methods

2.1 Plant materials and growth conditions

An *At4g11960* (*PPP7B*) insertion mutant line was identified in the SALK collection (http://signal.salk.edu/; Alonso *et al.*, 2003) which is made up of flank-tagged ROK2 T-DNA lines (ecotype Columbia-0). The *At4g22890* (*PPP7A*) insertion mutant line derives from the Sail collection (Session *et al.*, 2002), which is made up of a flank-tagged DAP101 T-DNA lines (ecotype Columbia-0). Both lines were identified by searching the insertion flanking database SIGNAL (http://signal.salk.edu/cgi-bin/tdna express).

pgr5 mutant seeds were kindly provided by Toshiharu Shikanai (Graduate School of Agriculture, Kyushu University Fukuoka, Japan). *Arabidopsis thaliana* wild-type (ecotype Columbia 0) and mutant seeds were sown in Petri dishes on water soaked Whatman paper and incubated three days at 4°C in the dark to break dormancy. Plants were gown on soil under greenhouse controlled conditions (PDF: 70-90µEm^{-2}s^{-1}, 16h light: 8h dark cycles). Fertilization with "Osmocote Plus" (Scotts Deutschland GmbH, Nordon Germanz) was performed according to manufacturer's instructions.

2.2 Complementation of *ppp7ab* mutant

The *PPP7A* and *PPP7B* complete coding regions (primers: P7AF: 5'- ATGGGTAGCA AGATGTTGTT-3'; P7AR: 5'-TTAAGCTTGGCTTCCTTCTGG-3'; P7BF: 5'-ATGGCTTTTACTCTAACAAT -3'; P7BR: 5'- TTAAGCTTTCCCTCCTTCTG -3') were ligated into the plant expression vector pH2GW7 (Invitrogen) under the control of a single Cauliflower Mosaic Virus 35S promoter and the constructs were used to transform flowers of *ppp7ab* mutant plants by the floral dipping technique as described in Clough and Bent (1998). Hygromycin resistant plants, selected *in vitro*, were transferred into the greenhouse and seeds were collected after 3 weeks. Successful complementation was confirmed by chlorophyll fluorescence measurement and P$_{700}$ oxidation state analysis (see below). In addition, the integration of the transgene in the genome of the complemented mutant plants was confirmed by PCR using specific primers (22890F: 5'-CTAAAGCCACAACAGAGCAATC-3' and 22890R: 5'-TGTAATGTCGTCCAGGAA-3'; 11960F: 5'-TACTCTAACAATCCCTAGATT-3' and 11960R: 5'-CCTCCT

_____

TCTGGTAATGTGATC-3') and the presence of the PPP7 protein was tested probing with specific antibodies thylakoid isolations as described below.

2.3 <u>Nucleic acid analysis</u>

Arabidopsis genomic DNA was isolated grinding fresh material in grinding buffer (200 mM Tris (pH 7.5), 250 mM NaCl, 25 mM EDTA, 0.5% SDS) followed by isopropanol precipitation. T-DNA insertion junction sites were recovered by polymerase chain reaction (PCR) with the use of combinations of insertion-specific and gene-specific primers, and then sequenced by means of the sequencing service at the LMU München (http://www.genetik.biologie.uni-muenchen.de/sequencing). T-DNA primers specific for ROK2 were LBb1 (5'-GCGTGGACCGCTTGCTGCAACTC-3') and RBb1 (5'-TCAGTGACAACGTCGAGCAC-3'). T-DNA primer specific for DAP101 was LB1 (5'-GCCTTTTCAGAAATGGATAAATAGCCTTGCTTCC-3'). Primers specific for *At4g22890* were PPP7A1F (5'-CAAGATGCAGTCTCCGTAGT-3') and PPP7A1R (5'-GCTGGAGATTGACAGAATTGT-3'); for *At4g11960*, PPP7B1F (5'-TAACTCATCGT TATGTGATCGA-3') and PPP7B1R (5'-GTCCAAATTACACATGTAACAAG-3'); for *PGR5* (*At2g05620*), pg5841F (5'-AGGTGATCACTGAGTTTTGC-3') and pg5961R (5'-ATCAGACACAAGCAGAGAG-3'). For the latter, the PCR products were digested with *Dde*I in order to discriminate between WT and mutant plants.

To determine gene expression, total leaf or root RNA was extracted from fresh tissues using the TRIzol reagent (Invitrogen, Karlsruhe, Germany). First-strand cDNA synthesis was performed using the SuperScript™ III Reverse Transcriptase (Invitrogen, Karlsruhe, Germany), and reverse-transcriptase-mediated PCRs (RT-PCR) were performed, using primers specific for *At4g22890* (sense primer 5'-ATGGGTAGCAAGATGTTGTTTA-3', antisense primer 5'-CAACGGTTGCTGGAACATTC-3') and *At4g11960* (sense primer 5'-TTTACTCTAACAATCCCTAGATTT-3', antisense primer 5'-CCTCCTTCTG GTAATGTGATCA-3') as well as *ACTIN1*-specific primers as a control (sense primer 5'-TGCGACAATGGAACTGGAATG-3', antisense primer 5'-GGATAGCATGTGG AAGTGCATACC-3'). To determine the difference in the level of gene expression, Real Time PCR has been performed on cDNA using specific primers on *PPP7A*, *PPP7B* and *PGR5* genes (ppp7aF: 5'-TCCTGGACGACATTACAG-3' and ppp7aR: 5'-

_____

TGATTGATAAAGCCAGATAT-3'; ppp7BF: 5'-GGGAAGAAGTTGATAGCA-3' and
ppp7bR: 5'-ATCGCTTTCGCTTCGTAATA-3'; pgr5F: 5'-AGTTCCAATGATGAA
GAATG-3' and pgr5R 5'-GCAAAACTCAGTGATCACCT-3').

2.4 <u>Synthesis of antibodies against the PPP7 protein</u>

Antibodies recognising both proteins PPP7A and PPP7B have been raised against the N
terminal domain of PPP7A. The cDNA regions corresponding to the N-Terminus of
PPP7A (from aa 61 to aa 200, primers: IG7F: 5'-CACCGCCACAACAGAGCAATCAG-
3' and IG7R: 5'-TTATTTGAAATAATCTACAGCGAG-3') was cloned in the pET151-
Topo vector (Invitrogen). The expression of the protein in *E. coli* cells (BL21-star) was
induced with 1 mM IPTG at 16°C overnight in LB medium (Sambrook *et al.*, 1989). The
expressed truncated PPP7A protein was purified by means of its His-Tag using a Ni-
Agarose resin under denaturating conditions (Invitrogen) according to manufacturers'
instructions. The purified protein was then injected into the rabbits. Probing them on
thylakoids isolated from single *ppp7a* and *ppp7b* mutants, proved that the antibodies
recognized both proteins as expected from the high homology of the protein sequences.

2.5 <u>Chlorophyll fluorescence and spectroscopic measurements</u>

Chlorophyll fluorescence was measured *in vivo* on single leaves, using a PAM (pulse
amplitude modulation) 101/103 fluorometer (Walz, Germany) as described before by
Varotto *et al.* (2000b). Saturating pulses (800 ms) of white light (4500 $\mu E\ m^{-2}\ s^{-1}$) were
used to determine the maximum fluorescence in the dark (F_M) and after the illumination
(F_M') and the ratio (F_M - F_0)/F_M corresponds to F_V/F_M. A 20-min illumination with actinic
light (80 $\mu E\ m^{-2}\ s^{-1}$) served to drive electron transport between PSII and PSI before Φ_{II} and
qP were measured according to the formulas (F_M'-F_S)/F_M' and (F_M'-F_S)/(F_M'-F_0). NPQ was
measured after 20 min illumination with actinic light of different light intensity, from 80 to
2000 $\mu E\ m^{-2}\ s^{-1}$, as described in *Results*, and it was calculated as (F_M-F_M')/F_M'.

2.6 <u>Measurements of the redox state of P_{700} and of CEF to LEF transition</u>

Redox changes of P_{700} were measured by monitoring the absorbance at 810 nm and 860 nm
with a PAM 101/103 chlorophyll fluorometer (Walz) connected to a Dual Wavelength

_____

ED_P700DW emitter-detector unit as described by Schreiber *et al.* (1988). Oxidized P_{700} levels (ΔA) were recorded *in vivo* during actinic light illumination under different light intensities (from 70 to 800 $\mu E\ m^{-2}\ s^{-1}$). The maximum level of oxidised P_{700} (ΔA_{MAX}) was recorded during far red light illumination (720 nm, 50 $\mu E\ m^{-2}\ s^{-1}$). The P_{700} oxidation state was then calculated as $\Delta A/\Delta A_{MAX}$.

CEF-to-LEF transitions were measured as P_{700} redox kinetics in intact leaves with a flash spectrophotometer as described before (Nandha *et al.*, 2007). Actinic light driving LEF was provided by a green LED peaking at 520 nm, and P_{700} oxidation was measured at 820 nm (Breyton *et al.*, 2006). P_{700} was specifically excited by far-red light and the maximum extent of P_{700}^{+} was estimated from the kinetics of P_{700} oxidation as described (Joliot and Joliot, 2005).

2.7 <u>Pigment analysis</u>

Pigment content was analysed by reverse-phase HPLC as previously described in Färber *et al.* (1997). Leaf discs were weighted, frozen in liquid nitrogen and ground to powder. Pigments were extracted with 95% acetone. After short centrifugation, pigment extracts were filtered through a 0.2 μm membrane filter and used directly for HPLC analysis performed in collaboration with Prof. Dr. Peter Jahns (Düsseldorf, Germany).

2.8 <u>Immunoblot analyses</u>

Leaves from 4-week-old plants were harvested and grinded in buffer 1 (0.4 M sorbitol, 0.1 M Tricine (pH 7.8-KOH) and 0.5% milk). After sieving the material through two layers of Miracloth (Calbiochem) to remove cellular debris, chloroplasts were collected centrifuging at 2,450 g for 5 min at 4°C in a Ja-25.50 (Beckman) rotor. The chloroplasts were resuspended and lysed in buffer 2 (20 mM Hepes (pH 7.8-KOH) and 10 mM EDTA) and thylakoids were collected by centrifugation at 12,000 g at 4°C for 10 min. Thylakoids were resuspended in storage buffer (10 mM Hepes (pH 7.5-KOH), 1 mM EDTA and 50% glycerol) and the chlorophyll concentration was determined measuring the absorbance at different wavelengths (A_{750}, $A_{663.6}$ and $A_{646.6}$) after acetone precipitation as described in Porra, 2002. Thylakoids or total chloroplasts (see paragraph **2.10**) were resuspended in two volumes of SDS-loading buffer (6 M Urea, 50 mM Tris-Cl (pH 6.8), 100 mM

_____

dithiothreitol, 2% SDS, 10% glycerol, 0.1% bromophenol blue) and subsequently loaded on acrylamide Tris-Tricine SDS-PAGE gradient gels (10 to 16% acrylamide) and fractionated according to Schaegger and Jagow (1987). After overnight run at 100 V (12-20 mA, anode buffer: 0.2 M Tris-Cl (pH 8.9), cathode buffer: 0.1 M Tris-Cl (pH 8.9), 0.1 M Tricine (pH 8.9), 0.1% SDS, 1 mM EDTA) the proteins were transferred to PVDF membranes by means of semi-dry blotting apparatus (Biorad) according to Towbin *et al*. (1979) using a current corresponding to 1 mA cm^{-2} in transfer buffer (96 mM Glycine, 10 mM Tris, 10% $^V/_V$ methanol).

Filters were then probed with antibodies against individual subunits of PSI, PSII and cyt b_6/f according to standard protocols (Sambrook *et al.*, 1989) and signals were detected by enhanced chemo-luminescence (ECL kit, Amersham Biosciences). The PGR5 protein was detected using antibodies gently provided by Toshiharu Shikanai (Fukuoka, Japan).

Both PPP7A and PPP7B proteins were detected by antibodies raised against the N terminal part of PPP7A protein (see paragraph **2.4**).

2.9 <u>Total protein preparation</u>

Leaves from 4-week-old plants were harvested and homogenized in solubilisation buffer (100 mM Tris (pH 8), 50 mM EDTA (pH 8), 0.25 M NaCl, 1 mM DTT and 0.7% SDS). The homogenate was heated at 65°C for 10 min and centrifuged at 16,000 g 10 min (at RT) to remove cellular debris. Prior electrophoresis fractionations, proteins were precipitated with ice-cold acetone following standard protocols (Sambrook et al., 1989) and resuspended in SDS-loading buffer (6 M Urea, 50 mM Tris-Cl (pH 6.8), 100 mM dithiothreitol, 2% SDS, 10% glycerol, 0.1% bromophenol blue).

2.10 <u>Isolation of intact chloroplasts</u>

Leaves of 4- to 5-week-old plants were homogenized in the homogenization buffer (330 mM sorbitol, 20 mM Tricine (pH 7.6), 5 mM EGTA, 5 mM EDTA, 10 mM $NaHCO_3$, 0.1% BSA and 330 mg/L ascorbate) and the homogenate was filtrated through two layers of Miracloth (Calbiochem). Chloroplasts were collected by a centrifugation at 2,000 g for 5 min at 4°C. The pellet was carefully resuspended in the washing buffer (330 mM sorbitol, 20 mM HEPES/KOH (pH 7.6), 5 mM $MgCl_2$ and 2.5 mM EDTA). Chloroplasts were

loaded on a two-step Percoll gradient as described in Aronsson and Jarvis (2002). Intact chloroplasts at the interface between the two Percoll phases were broken by incubation for 30 min on ice in four volumes lysis buffer (20 mM HEPES/KOH (pH 7.5), 10 mM EDTA) and used for subsequent experiments. To separate thylakoids and stroma phases, ruptured chloroplasts were centrifuged at 42,000 g, 30 min at 4°C.

2.11 PSI isolation

Leaves from 4-week-old plants were harvested and thylakoids were prepared following the protocol described in paragraph **2.8**. Thylakoids were washed twice in 5 mM EDTA (pH 7.8) and dilute to 2 mg mL^{-1} chlorophyll concentration. An equal volume of 2% n-dodecyl-β-D-maltoside (β-DM) was added to the thylakoids and solubilisation was carried out on ice for 10 min. The un-solubilised part was pelleted by centrifugation at 16,000 g for 5 min at 4°C and the supernatant was loaded on a sucrose gradient (prepared directly into the centrifuge tubes after a freezing-thawing cycle of a 0.4 M sucrose, 20 mM Tricine (pH 7.5), 0.06% β-DM solution). The gradients were centrifuge at 191,000 g (SW40 rotor) for 21 h at 4°C. The PSI migrated as a distinct band on the bottom of the gradient. PSI isolations were separated in 16% to 23% acrylamide Tris-Glycine SDS-PAGE following standard protocols (Sambrook *et al.*, 1989).

2.12 *In vitro* assay of ferredoxin-dependent plastoquinone reduction

Ferredoxin-dependent plastoquinone reduction was measured in ruptured chloroplasts diluted in lysis buffer (see paragraph **2.10**) to 10 µg Chl mL^{-1} and immediately used for the measurements of chlorophyll fluorescence with a PAM fluorometer 101/103 (Walz, Germany). The fluorescence increase after the addition of 5 µM spinach ferredoxin (Sigma) and 0.25 mM NADPH (Sigma) was recorded under measuring light corresponding to 1 µE m^{-2} s^{-1}.

2.13 *In vitro* import in pea chloroplasts

Coding regions for *PPP7A* and *PPP7B* were amplified by PCR (using the primers ppp7aFimp: 5'- ATGGGTAGCAAGATGTTGTT-3', ppp7aRimp: 5'-TTAAGCTTGGC TTCCTTCTG-3'; ppp7bFimp: 5'-ATGGCTTTTACTCTAACAATCCC-3', ppp7bRimp:

_____

5'-TTAAGCTTTCCCTCCTTCTGGTA-3') and cloned into pGEM-Teasy vector (Promega, Madison, USA) under control of the T7 promoter. The constructs were verified by DNA sequencing (http://www.genetik.biologie.uni-muenchen.de/sequencing). mRNA was obtained by transcription with T7-RNA polymerase according to manufacturer's instructions (MBI Fermentas, St. Leon-Rot, Germany) and used for translation in wheat germ (Wheat Germ Extract System, Promega, Madison, USA) in the presence of [^{35}S]methionine at 30°C for 1 h. Transcription of pSSU and pOE33 constructs (gift from Jürgen Soll, Germany) was performed from the SP6 promoter and proteins were synthesized in Reticulocyte Extract System (Flexi®, Promega, Madison, USA) as outlined above. All translation mixtures were centrifuged at 50,000 g for 1 h at 4°C prior to import experiments.

Intact chloroplasts were isolated from 10-day-old pea leaves (*Pisum sativum*, var. Golf) and purified through Percoll density gradients as described (Waegemann and Soll, 1991). Import assays were performed with chloroplasts equivalent to 20 µg of chlorophyll in 100 µl of import buffer (10 mM methionine, 10 mM cysteine, 20 mM potassium gluconate, 10 mM NaHCO$_3$, 330 mM sorbitol, 50 mM HEPES/KOH (pH 7.6), 5 mM MgCl$_2$) (Nada and Soll, 2004). The amount of translation product never exceeded 10% of the total reaction volume. The import was carried out at 25°C for 30 min. Chloroplasts were subsequently re-purified over a 40% Percoll cushion in import buffer. If no additional treatment was intended, the chloroplasts were washed twice (30 mM sorbitol, 50 mM HEPES (pH 7.6), 0.5 mM CaCl$_2$) and samples for SDS-PAGE were prepared adding two volumes of SDS-loading buffer (described in paragraph **2.9**). For thermolysin treatment, chloroplasts were washed in 330 mM sorbitol, 50 mM HEPES (pH 7.6), 0.5 mM CaCl$_2$ and incubated with 20 µg/mL thermolysin (Calbiochem, Darmstadt, Germany) for 20 min on ice. The reaction was stopped by addition of EDTA (pH 8) to a final concentration of 5 mM and chloroplasts were washed once again. The treatment with trypsin (10 µg/mL) was performed for 30 min on ice and the reaction was stopped by adding two volumes SDS sample buffer (6 M Urea, 50 mM Tris-Cl (pH 11), 100 mM dithiothreitol, 2% SDS, 10% glycerol, 0.1% bromophenol blue). When indicated, the chloroplasts were incubated with 10% β-DM before trypsin treatment.

_____

To obtain membrane fraction, chloroplasts were hypotonically lysed in 50 mM HEPES/KOH (pH 7.6) and membranes were collected after centrifugation at 10,000 g for 10 min at 4°C. Treatment with 6 M urea was carried out in 50 mM HEPES/KOH (pH 7.6) for 15 min at 25°C (Nada and Soll, 2004). Solubilised proteins were separated from the insoluble fraction after centrifugation at 10,000 g for 10 min at 4°C.

To fractionate envelope, stroma and thylakoids, after import and thermolysin treatment, chloroplasts were washed twice as before and resuspend in 20 mM Tricine (pH 7.6), 5 mM MgCl$_2$. The lysis was conduced on ice for 30 min and the lysate was loaded on a two-step sucrose gradient (15% and 35% sucrose, prepared in Tricine buffer) and centrifuged for 3 h at 134,000 g at 4°C. Stromal fraction (upper part) was precipitated with ice-cold TCA (final concentration: 10%), washed twice with ice-cold acetone and resuspended in SDS-PAGE loading buffer. The envelope fractions, distributed in the middle of the gradient, were centrifuged at 280,000 g, 4°C for 30 min and resuspended in SDS-PAGE loading buffer. The thylakoid fraction (pelletted at the bottom of the gradient) was directly resuspended in SDS loading buffer.

Radiolabelled proteins were separated by SDS-PAGE and detected with a PhosphoImager (FujiFilm FLA-3000).

2.14 Intracellular localization of dsRFP fusion in *Arabidopsis* protoplasts

Coding regions of *PPP7A* and *PPP7B* genes were amplified by PCR (using the primers ppp7aFRFP: 5'- CACCATGGGTAGCAAGATGTTGTT-3', ppp7aRRFP: 5'-AGCTTG GCTTCCTTCTG-3'; ppp7bFRFP: 5'-CACCATGGCTTTTACTCTAACAA-3', ppp7bR RFP: 5'-AGCTTTCCCTCCTTCTGGTA-3') and cloned upstream of the dsRED sequence in the pGJ1425 vector by digestion with *Nco*I (Jach *et al.*, 2001). Sterile cotyledons of 2-week-old *Arabidopsis* plants (ecotype Col_Gl-1) were cut and incubated for 16 h at 24°C in the dark in a protoplasting solution 1 (10 mM MES, 20 mM CaCl$_2$, 0.5 M mannitol, pH 5.8, 0.1 g/mL macerozyme (Duchefa), 0.1 g/mL cellulase (Duchefa)). Protoplasts were collected by centrifugation at 50 g for 10 min. Protoplasts were resuspended in 8 mL of solution 2 (10 mM MES, 20 mM CaCl$_2$, 0.5 M mannitol, 120 g/L sucrose, pH 5.8). 2 mL of solution 3 (10 mM MES, 10 mM CaCl$_2$, 10 mM MgSO$_4$, 0.5 M mannitol, pH 5.8) were added on top of the protoplasts and intact protoplasts were recovered at the interface

_____

between the two solutions after centrifugation at 70 g for 10 min (described in Dovzhenko *et al.,* 2003). 40 μg of plasmid DNA were introduced into protoplasts by PEG transfection in the solution (40 % PEG solution, 70 mM $Ca(NO_3)_2$). PEG solution was prepared dissolving 0.413 g $Ca(NO_3)_2 \cdot 4H_2O$, 1.275 g mannitol and 10 g PEG 1500 (Merck, Germany) in 17.5 ml H_2O (described in Koop *et al.,* 1996). Microscopy analysis (with Fluorescence Axio Imager microscope in ApoTome mode (Zeiss)) was conducted after 16 h of incubation at 23°C in the dark. Fluorescence was excited with the X-Cite Series 120 fluorescence lamp (EXFO) and images were collected in the 565-620 nm (dsRED fluorescence) and 670-750 nm (chlorophyll auto-fluorescence) ranges.

2.15 2D Blue Native/SDS PAGE for thylakoids protein analysis

Leaves from 4-week-old plants were harvested and thylakoids were prepared as described in paragraph **2.8**. For the first dimension of Blue Native PAGE analysis, protein amounts equivalent to 100 μg of chlorophyll for each genotype were washed with 10 mM Tris-HCl (pH 6.8), 10 mM $MgCl_2$ and 20 mM KCl, and subsequently solubilised in 750 mM ε-aminocaproic acid, 50 mM Bis-Tris (pH 7.0), 5 mM EDTA (pH 7.0), 50 mM NaCl and 1.5% $^W/_V$ β-DM. Solubilized samples were then incubated for 1 h on ice and afterwards centrifuged for 10 min at 21,000 g and 4°C. Supernatants were supplemented with 5% $^W/_V$ Coomassie-blue in 750 mM ε-aminocaproic acid, and directly loaded onto BN gels (4-12% acrylamide gels, containing 0.5 M ε-aminocaproic acid, 50 mM Bis-Tris (pH 7.0) and 10% glycerol). One dimensional BN-PAGE was carried out at 750 V and 12 mA with cathode buffer (50 mM Tricine, 15 mM Bis-Tris (pH 7.0) and 0,02% Coomassie G) and anode buffer (50 mM Bis-Tris (pH 7.0)) as described by Schägger and von Jagow (1991). The gel slices corresponding to the first dimension were treated in denaturing buffer (0.125 M Tris-Cl (pH 6.8), 4% SDS and 1% β-mercaptoethanol) for 30 min at room temperature and 5 min at 70°C before the second dimension run. Second dimension was performed as described in paragraph **2.8.**

2.16 Yeast two hybrid and split ubiquitin assay

For yeast two hybrid assay, coding sequences of mature bait proteins (without cTP, for a list of primers that have been used, refer to **Table 2.1**) were cloned into pGBKT7 carrying

_____

the GAL4 DNA-binding domain and the pGADT7 vector (described in Harper *et al.*, 1993), carrying the GAL4 activation domain, was used to express the prey proteins. YPAD (6.0 g yeast extract, 12 g peptone, 12 g glucose, 6 g adenine hemisulphate: dissolve in 600 ml distilled water), SC (4 g yeast nitrogen base, 12 g glucose, 0.5 g synthetic complete drop out mix: dissolve in 600 ml distilled water) and synthetic complete drop out mix (mix 2 g adenine hemisulfate, 2 g arginine-HCl, 2 g histidine-HCl, 2 g isoleucine, 2 g leucine, 2 g lysine-HCl, 2 g methionine, 3 g phenylalanine, 6 g homoserine, 3 g tryptophan, 2 g tyrosine, 1.2 g uracil, 9 g valine) have been described previously by Sherman (1991). The yeast two hybrid assay was performed as described in James *et al*. (1996) using the yeast strain AH109 supplied by Clontech (Palo Alto, CA).

For split ubiquitin assay, the coding sequence of the mature PPP7A protein was cloned in pAMBV4 and used as bait in interaction studies with prey proteins which were generated by cloning the coding sequences of mature thylakoid proteins into pADSL (for a list of primers, refer to **Table 2.2**). Interaction studies were performed using the Dual-Membrane kit (Dualsystems Biotech AG) according to manufacturer's instruction and as described by Pasch *et al.* (2005).

Sequence Name	Sense primer	Antisense primer
PPP7A N-Terminus	acggaattcgccacaacagagcaatcaggtcca	aggtcgacggattttgaaaataatctacagcgag
PPP7A C-Terminus	acggaattcgacttcttgatcttgaagggtcct	aggtcgacggatagcttggcttccttctggcaa
FNR1 (At5g66190)	gccgaattcgatactaccgaggcaccaccagt	gcaggtcgacgttagtagacttcaacattcc
FNR2 (At1g20020)	gccgattcgaaacagatactcctactcc	gcaggtcgactcagtagacttcaacgttcc
psaE1 (At4g28750)	ccgaattcgtcacctcggtcgccggcgct	aggtcgacgttaagctgcaacttcttcga
psaD1 (At1g03130)	ccgaattcaccactacttccgccgtcaag	aggtcgacttacaaatcataagattgtttc
Fd (At1g60950)	gccgaattcgctacatacaaggtcaagttc	caggtcgacgttaaacaatgtcttcttcttt

Table 2.1 List of primers (5' to 3' orientation) used for cloning pray and bait sequences for yeast two hybrid assay.

_____

Sequence Name	Sense primer	Antisense primer
pgr5 (At2g05620)	gctggatccatggctgctgcttcgtttc	gagaattcctaagcaaggaaaccaagc
PPP7A	cgctctaagaatgggtagcaagatgttgtt	cgcaggcctgcttggcttccttctggca
FNR1 (At5g66190)	acggatccacaacagatactaccgaggca	tatcgaattctcttagtagacttcaacattcca
FNR2 (At1g20020)	acgcccgggaaacagaaacagatactcct	tatcgaattctctcagtagacttcaacgttcc
psaE1 (At4g28750)	gctggatccgtcacctcggtcgccggcgct	tcgaattctcttaagctgcaacttcttcgac
psaD1 (At1g03130)	gctggatccaccactacttccgccgtcaag	tcgaattctcttacaaatcataagattgtttc
CytB (PetB) pAMBV4	cgtctagaaaaaatgagtaaagtttatgattg	gcccatggagtaagggaccagaaataccttg
CytB (PetB) pADSL	cgtggatccatgagtaaagtttatgattg	tcgaattctcttataagggaccagaaatacc
Fd (At1g60950)	ctgggatccgctacatacaaggtcaagttca	tatcgaattctcttaaacaatgtcttcttctttg

Table 2.2 List of primers (5' to 3' orientation) used for cloning pray and bait sequences for the split ubiquitin assays.

For both interaction analyses positive and negative controls were used, as listed in the following tables.

Yeast Two Hybrid	
Empty BD	PGR5-AD
PGR5-BD	Empty AD
Empty BD	Fd-AD
Empty BD	FNR1-AD
Empty BD	FNR2-AD
Empty BD	PSI D-AD
c-PPP7-BD	Empty AD

| Split Ubiquitin	
PPP7-Cub	pADSL-Nx
PPP7-Cub	Alg5-NubG
PPP7-Cub	Alg5-NubI
pAMBV4	PGR5-NubG
pAMBV4	Fd-NubG
pAMBV4	FNR1-NubG
pAMBV4	FNR2-NubG
pAMBV4	Cyt b_6-NubG
pAMBV4	cpSRP43-NubG
pAMBV4	PSII D1-NubG
pAMBV4	suIV-NubG
Cyt b_6-Cub	pADSL-Nx
Cyt b_6-Cub	Alg5-NubG
Cyt b_6-Cub	Alg5-NubI

3. Results

## 3.1 <u>Gene structure and homologies</u>

Previous work identified groups of transcriptionally co-regulated nuclear genes in *Arabidopsis thaliana*, which were enriched for photosynthetic genes (Biehl *et al.*, 2005). These photosynthetic regulons contain genes of yet unknown function, the products of which represent putative photosynthetic proteins (PPPs). One of them, PPP7, is the subject of this thesis.

PPP7 is encoded by the two highly homologous genes *At4g22890* (*PPP7A*) and *At4g11960* (*PPP7B*), that are located on a duplicated region of chromosome 4 of *A. thaliana*. The PPP7 proteins do not share any common motive with proteins of known function, but are conserved among different species. Orthologous genes can be found in flowering plants both in monocotyledons like *Oryza sativa* and *Zea mays*, and in dicotyledons for instance *Populus trichocarpa* and *Lycopersicon esculentum* (**Figure 3.2**). Also the eukaryote algae *Chlamydomonas reinhardtii* and the moss *Physcomitrella patens* possess an orthologue of *PPP7*.

When analyzing the publicly available microarray data of *A. thaliana* (https://www.geneve-stigator.ethz.ch/) both genes, *PPP7A* and *PPP7B*, showed an increased expression in green tissues. This could be confirmed by Real-Time PCR on cDNA extracted from leaves and roots of wild type (WT) plants (**Figure 3.1**). Additionally, it can be observed that the expression level of *PPP7A* is considerably higher than the expression level of *PPP7B*.

Fig 3.1. Real-Time PCR analysis on cDNA from leaves and roots of WT plants using specific primers on *At4g22890* and *At4g11960*. The expression levels are shown as arbitrary units, normalized on the expression levels of *ACTIN 1* which was used as a reference.

```
PPP7A              MGSKMLFSLTSPRLFSAVSR--KESSSFSPSPPSESSRTQWTQ-LSPGKSISLRRR  53
PPP7B              ----MAFTLTTPR-FSAISR--KPITCSSSRTQCEAP-------FTHGRSISLRRR  42
Os08g0526300       ----MASLLPSBVFPTAAAAAASTSSSSRCRCRCRITTSSSAHGWSNCQGWRLHHR  52
Os03g0857400       ------MLMASEAWLSPASRLFHPPRSSTAAFFSASGLPRLPRRSSCALATSIRGR  50
P. trichocarpa gw1 MAGKLAFTLTSPRVLIAPIQ--KPFISSSSSLPPESC-SSSTRVHFNVKQFSLRRR  53
P. trichocarpa gr3 MASKLAFNLTSPRVFIAPIQ--KPIISSSSSLPSLSSPSCSTRVQLNGKQFSLRGR  54
C. reinhardtii     ----MQTTVLRSSTRVGCVR---EVGLARALPVRF------------VVFGSRTP  36
```

```
PPP7A              VFLLPAKAT----TEQS-GPVG-GDNVDSNVLPYCSINKA----EKKTIGEMEQEFLQALQSFYY  108
PPP7B              LTLLPLKAS----TDQS-GQVG-GEEVDSKLLPYCSINKN----EKRTIGEMEQEFLQAMQSFYY   97
Os08g0526300       VWAAQAADQQGGVQQQQQQEENEDGVVDSNVLPYCSINRK----EKKTIGEMEQEFLQALQAFYY  113
Os03g0857400       RLRIGATDQ-----QQQQGKQDGDEVVDSNVLQYCSIDGKGKKAEKRSLGEMEQEFLQALQAFYY  110
P. trichocarpa gw1 MLLPPTKAT----ADQQAGLX--DEMVDGKILQYCSIDKR----GKKSIGEMEQEFLQALQAFYY  108
P. trichocarpa gr3 MLFLPTKAT----ADQQTDVQEDMDDGKILQYCSIDKK----GKKSLGEMEQDFLQALQAFYY  111
C. reinhardtii     MLLRSAKKD--------DGYISEDEGLGNVAADYCAIDGAG-KKAKRSLGEMEQEFIAAMTSWYY   92
```

```
                   *        ** *    **   *        **   *            *** *
PPP7A              DGKAIMSNEEFDNLKEELMWEGSSVVMLSSDEQRFLEASMAYVSGNPILNDEEYDKLKLKLKIDG  173
PPP7B              EGKAIMSNEEFDNLKEELMWEGSSVVMLSSDEQRFLEASMAYVSGNPILSDEEYDKLKMKLKMDG  162
Os08g0526300       DKKAVMSENEFDNLKEELMWEGSSVVMLSPDEQRLLEASMAYVAGNPIMTDAEFDELKLRLRKEG  178
Os03g0857400       DQKAIMSNEEFDNLKEELMWEGSSVVMLSPDEQRLLEASMAYAAGNPIMSDAEFDQLKLRLKKDG  175
P. trichocarpa gw1 EGKAIMSNEEFDNLKEELMWEGSSVVMLSSDEQKFLEASMAYVSENPIMSDKEYDLKMKLKSEG  173
P. trichocarpa gr3 EGKAIMSNEEFDNLKEELMWQGSSVVMLSSDEQKFLEASLAYVSGNPIMNDEEFDKLKIKLKTEG  176
C. reinhardtii     EGKPTMSDEEFSLLKEELIWSGSMVAVLSSDEQRFLEASMAYAKGKPIMTDEDYDALKAELRNKS  157
```

```
                                                         TM1
PPP7A              SDIVSEGPRCSLRSKKVYSDLAVDYKMLLLNVPATVVALGLFFFLDDITGFEITYIMELPEPYS  238
PPP7B              SEIVCEGPRCSLRSKKVYSDLAIDYFKMFLLNVPATVVALGLFFFLDDITGFEITYLLELPEPFS  227
Os08g0526300       SEIVQEGPRCSLRSRKVYSDLTVDYFKMFLLNVPAAVLALTLFFFLDDITGFEITYLLELPEPFS  243
Os03g0857400       SDIVTEGPRCSLRSRKVYSDLTVDYLKMFLLNVPATTLALGLFFFIDELTGFEIN-IFQLPEPFG  239
P. trichocarpa gw1 SEIVVEGPRCSLRSRKVYSDLYVDYLKMFLLNVPATVTALGLFFFLDDLTGFEITYLLELPEPFS  238
P. trichocarpa gr3 SEIVVEGPRCSLRSRKVYSDLSVDYLKMFLLNVPATVVALGLFFFLDDLTGFEITYLLELPEPFS  241
C. reinhardtii     SIVTAQGPRCSIRSKKMYADAEPDYLRMTALNIPGVLFVLGIVFAVDYSTGFGVTKLVELPAPYG  222
```

```
                   TM2
PPP7A              FIFTWFAAVPVIVYLALSITKLIIKDFLILKGPCPNCGTENISFFGTILSISSGGKTNTVKCTNC  303
PPP7B              FIFTWFAVPAIVYLALSLTKLILKDFLILKGPCPNCGTENVSFFGTILSIPNDSNTNNVKCSGC  292
Os08g0526300       FIFTWFAALPLIFWVAQALTSAIVKDFLILKGPCPNCGNENLSFFGTILSVPSGGARNSVKCANC  308
Os03g0857400       FIFTWFAALPLILFIAQSITNAIVNDFLILKGPCPNCGAENLSFFGTILSVSSGGETNKVKCADC  304
P. trichocarpa gw1 FLFTWFAAVPLIVWLALTLTNAIVKDFLILKGPCPNCGTENGSFFGTILSISSGGTTNTLKCSNC  303
P. trichocarpa gr3 FLFTWFAAVPLIVWLALTLTNAIVKDFLILKGPCPNCGTENGSFFGTILSISSGGASNTLKCSNC  306
C. reinhardtii     PILLWGLLLPLSLFTVAYALTCVGFKDNLILKAPCPSCGSENFSYFGDVFTVAGARGQNLVECPNC  287
```

```
PPP7A              GTAMVYDSGSRLITLPEGSQA----------------------  324
PPP7B              GTEMVYDSGSRLITLPEGGKA----------------------  313
Os08g0526300       SSSLVYDSASRLITLPETAEA----------------------  329
Os03g0857400       STEMVYDSKSRLITLPEPSQ----------------------  324
P. trichocarpa gw1 STELVYNSKTRLITLPEGSEA----------------------  324
P. trichocarpa gr3 STELVYDSKTRLITLPEGSEA----------------------  327
C. reinhardtii     KADMIFDEYKRVVVVAETSEVKQEKLAAAAAKKAAAAAKKKAKAAA  333
```

Fig 3.2. Sequence alignment of the PPP7 proteins in *A. thaliana* and other plant and algal species. Chloroplast transit peptides are indicated in italics, predicted transmembrane domains are boxed. A putative negatively charged region is indicated by asterisks. The alignment has been created with the program Clustal W (http://www.ebi.ac.uk/clustalw/) and sequences have been obtained from the genome sequences available at http://genome.jgi-psf.org/ and http://www.ncbi.nlm.nih.gov/.

## 3.2 <u>PPP7A and PPP7B are targeted to the thylakoid membrane</u>

Already a few years ago, Peltier *et al.* (2002) identified PPP7A as a component of the chloroplast proteome by using mass spectrometry. In 2004, Kleffmann *et al*. confirmed the chloroplast localization of PPP7A, while Friso *et al*. (2004) found PPP7A to be a thylakoid transmembrane protein. To analyze the localization of PPP7 proteins, three different techniques have been applied.

A first *in silico* approach clearly showed that the gene products of both *PPP7A* and *PPP7B* are predicted to be targeted to the chloroplasts by at least five of seven publicly available predictor algorithms (**Table 3.1).**

	ChloroP	TargetP	Predotar	Mitoprot	iPSORT	PCLR	PSORT
PPP7A	C (0.598)	C (0.956)	C (0.770)	M (0.985)	M	C (0.999)	C (0.888)
PPP7B	C (0.557)	C (0.904)	C (0.670)	M (0.993)	C	C (0.874	M (0.845)

Table 3.1. *In silico* prediction of subcellular targeting of PPP7A and PPP7B. In parentheses the highest output scores for each program are reported. C: chloroplast; M: mitochondrion.

The second approach was the *in vivo* localization of PPP7A and PPP7B in *Arabidopsis* protoplasts: the full-length coding sequences of both genes have been fused 5' to the sequence coding for the red fluorescence protein of the coral *Discosoma* (dsRFP; described in Jach *et al.*, 2001). The obtained constructs were used to transiently transfect *Arabidopsis thaliana* (ecotype C24) protoplasts. The signal of both RFP-fusion proteins is clearly associated with the chloroplasts and overlaps with the signal of chlorophyll auto-fluorescence (**Figure 3.3**).
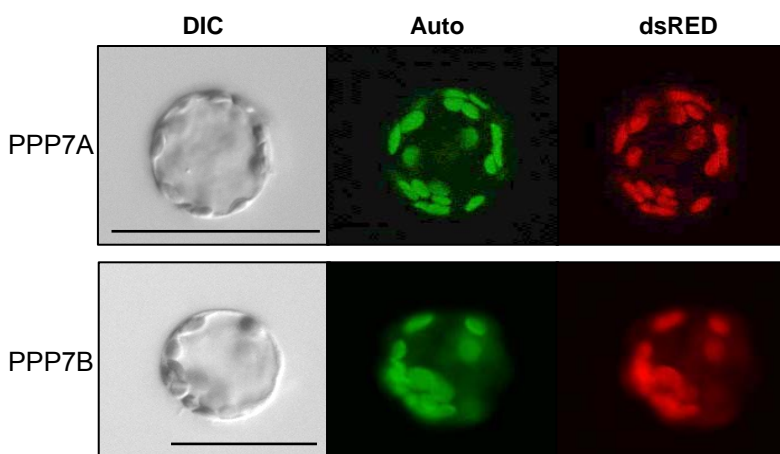
Fig 3.3. Subcellular localization of the PPP7 proteins. The *PPP7A* and *PPP7B-dsRED* fusions were transiently expressed in *Arabidopsis* protoplasts and protein localization was analyzed using fluorescence microscopy. "DIC": differential interference contrast image; "Auto": chloroplasts revealed by chlorophyll auto-fluorescence; "dsRED": dsRED protein-fluorescence.
Scale bars = 50 μm.

Considering that PPP7A and PPP7B are expected to contain two transmembrane domains separated by a loop of 19 aminoacids (as predicted by the TMHMM program at http://www.cbs.dtu.dk/serv-ices/TMHMM-2.0/), *in vitro* import in pea chloroplasts served as third system to understand whether the two proteins are integrated into the thylakoid membrane. As shown in **Figure 3.4.A,** both PPP7A and PPP7B can associate with the chloroplast and be imported. After the import, a signal peptide is cleaved and the mature protein is protected from thermolysin inside the intact chloroplasts. Moreover, when chloroplasts are osmotically ruptured after import and fractionated into stromal phase, envelope and thylakoid membranes through a sucrose gradient, the radioactive signal stays within the thylakoid fraction (**Figure 3.4.B**). To understand if the PPP7s are integral or peripheral membrane proteins, chloroplasts were lysed after import and the membranes were collected and washed with 6 M urea. Urea is known to break hydrogen bonds and salt bridges responsible for protein-protein interactions (Semenova, 2001) and therefore to dissociate peripheral or loosely associated membrane proteins. The peripheral lumen-exposed thylakoid protein PSII-O, a component of the oxygen evolving complex has been used as a positive control and in fact is much more abundant in the soluble fraction. On the contrary, PPP7A is not present in the soluble fraction, but is predominantly found in the membrane fraction (**Figure 3.4.C**).
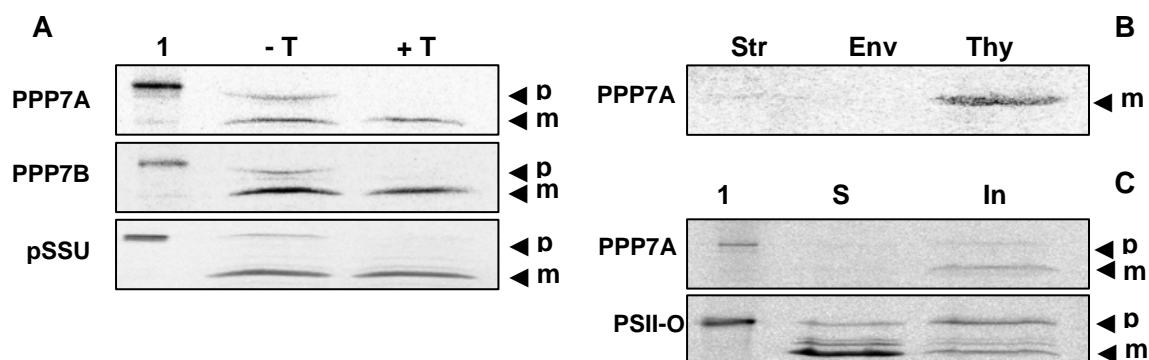
Fig 3.4. Subcellular localization of PPP7 proteins: **A**. ^{35}S-labelled PPP7A and PPP7B proteins, translated in vitro (lanes 1: 10% translation product) were incubated with isolated chloroplasts for 30 min at 25°C and chloroplasts were recovered by centrifugation through 40% Percoll (lane -T). Chloroplasts were incubated with 20 μg/mL thermolysin (lane +T), subjected to SDS-PAGE, and proteins were visualized by autoradiography. The small subunit of Rubisco (pSSU) was used as a positive control. p: precursor; m: mature protein. **B.** Chloroplasts were fractionated after import. Str: stroma; Env: envelope; Thy: thylakoids. **C**. After import of radio-labelled PPP7A and PSII-O proteins, chloroplasts were lysed and membranes were collected by centrifugation and treated with 6 M urea. Lanes **S** represent the solubilised proteins and lanes **In** the insoluble fraction. Lanes 1 represent 10% translation product, p and m indicate precursor and mature proteins.

Further evidence for the thylakoid localization of the PPP7s was provided by western analysis using antibodies against PPP7 on WT and *ppp7ab* chloroplasts, thylakoid and stromal fractions (**Figure 3.5**).
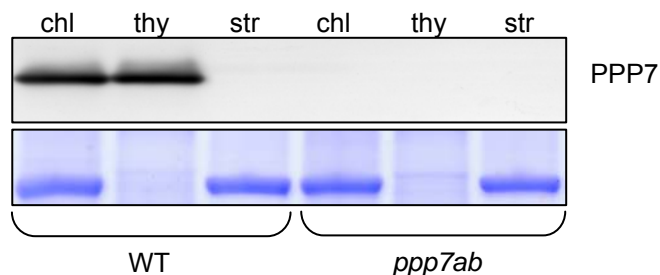
Fig 3.5. Subcellular localization of PPP7 proteins: **chl** lanes correspond to 5μg chlorophyll of intact chloroplasts; **thy** lanes correspond to the thylakoid fraction coming from the osmotic lysis of 5μg chlorophyll of chloroplasts and **str** lanes correspond to the stromal fraction of the same lysis reaction. In the lower panel, the Coomassie staining of the portion of the gel, where the large subunit of the Rubisco runs, is presented to confirm the purity of the fractions.

3.3 Topological orientation of PPP7 in the thylakoid membrane

According to predictions (see **Figure 3.2**), PPP7 proteins probably fold with two transmembrane helices separated by a loop of 19 aminoacids. Both N- and C- terminal domains of the protein represent hydrophilic regions of 141 and 63 aminoacids, respectively. As a result, two topological orientations of PPP7 can be assumed:

Topology 1   *Topology 2*
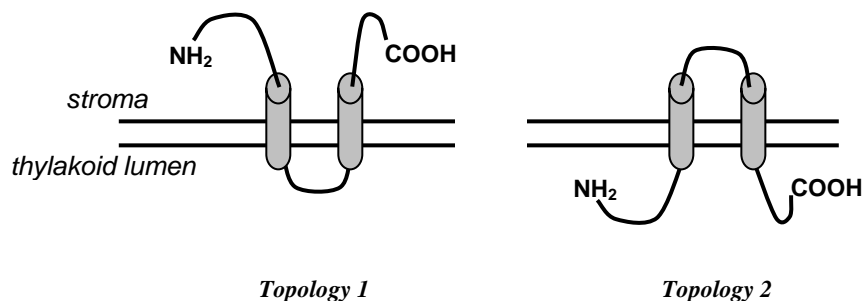
To understand the real topology of PPP7, mild trypsin digestion was applied to intact thylakoids. Trypsin hydrolyzes the peptidic bonds at the carboxylic groups of aminoacids arginine and lysine and is not permeable to membranes, for that it is digesting the part of the protein exposed to the stromal side of the thylakoids. Both the C-terminus and the N-terminus of the protein contain multiple trypsin cleavage sites (PeptideCutter, http://expasy.ch/tools/peptidecutter/), while the loop between the two does not carry any sequences predicted to be cleaved by trypsin. If the native PPP7 conformation is the topology

model 1, the N- and C- terminal domains are exposed to the stroma and they will therefore be digested by trypsin. In this case, a fragment of 6.7 kDa will remain protected, comprising the loop and the two transmembrane domains. If the protein is folded according to topology model 2, it would remain insensitive to the trypsin treatment, since the loop between the two membrane helices does not contain a single trypsin cleavage site.

The quality of the preparations was monitored by digestion pattern of the intermediate and mature form of the PSII-O subunit of the lumenal Oxygen Evolving Complex.
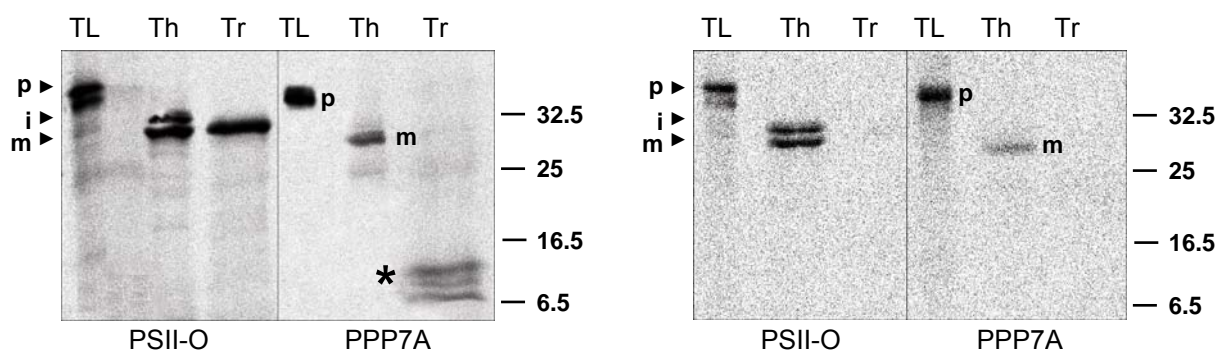
Fig 3.6. **Left**: Trypsin treatment of the thylakoid membrane with incorporated ^{35}S-PSII-O and ^{35}S-PPP7A. Pea chloroplasts corresponding to 20 μg of chlorophyll were incubated with ^{35}S-labeled pPSII-O and pPPP7A for 30 min. Intact chloroplasts were re-purified after import and treated with thermolysin to remove the precursor proteins (lane Th). Thylakoids were isolated and trypsin was added to 10 μg/mL (lane Tr). **Right**: Trypsin treatment of thylakoids after solubilisation with β-DM. Thermolysin treatment of chloroplasts after import (lane Th). Thylakoids were incubated with β-DM prior to trypsin treatment in order to release protein complexes from the membrane (lane Tr). Lanes TL represent 1/10 of the translation product. On the right side of both panels, the corresponding protein MWs are indicated in KDa.

Concerning the PSII-O control (**Figure 3.6**) the stromal intermediate protein, present in intact chloroplasts (Th lane), completely disappeared in the trypsin-treated thylakoids whereas the mature form of PSII-O remains intact and no partial proteolysis can be detected (Tr lane). Quite the opposite is the case for PPP7A. Its mature form is digested into three low-molecular-weight products (*), the smallest of them being approximately 7 kDa in size while the other two are ranging from 9 to 14 kDa. The appearance of a 7 kDa digestion product is in agreement with the topology 1 folding. The appearance of the two additional fragments of larger size may indicate higher resistance of certain PPP7 domains from trypsin digestion, possibly implying tight interactions of PPP7 with other protein constituents on the stromal side of the thylakoid membrane.

As an additional control, isolated thylakoids were treated with 10% n-dodecyl- β-D-maltoside (β-DM) prior to trypsin treatment in order to extract protein complexes from the thylakoid membrane. Both imported PSII-O and PPP7A were entirely degraded under those conditions (**Figure 3.6**), confirming that the observed protease resistance was due to the membrane barrier.

Eventually, the topology of the native PPP7s was studied by means of immunoblotting analysis. Anti-PPP7 antibodies were raised against the first 140 N-terminal amino acids of the mature PPP7A protein and recognize both PPP7A and PPP7B (**Figure 3.9**). If the conclusion that the N-terminal region is exposed to the stromal side was correct, PPP7 should be no longer detectable by anti-PPP7 antibody after trypsin treatment of thylakoid membrane. Indeed, the PPP7 signal was barely visible after trypsin treatment (**Figure 3.7**).
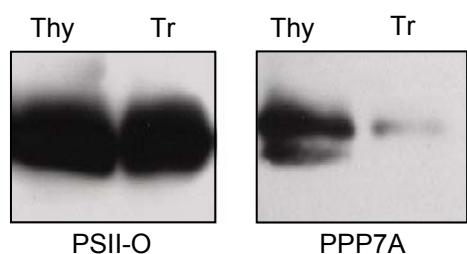
Fig 3.7. Immunoblotting of the thylakoid membrane with α PsbO and α PPP7 antisera before (lane Thy) and after (lane Tr) trypsin treatment.

3.4 *ppp7a* and *ppp7b* mutations

The gene structures of *PPP7A* and *PPP7B* are depicted in **Figure 3.8.A**. The predicted intron-exon organization was confirmed by RT-PCR for both genes and the sequences obtained were compared with the coding sequences available on public websites (MIPS: http://mips.gsf.de/proj/plant/jsf/athal/searchjsp/index.jsp and TAIR: http://www.arabid-opsis.org/). T-DNA insertion mutants for *PPP7A* and *PPP7B* were identified by browsing a T-DNA insertion flanking database (http://signal.salk.edu/cgi-bin/tdnaexpress). For each of the two genes, a single mutant line could be identified, the SAIL line Sail_443E10 mutated in *PPP7A* and the Salk line Salk_059233 for *PPP7B*. For both lines the insertion site has been determined using gene- and T-DNA-specific primers, followed by sequencing of the PCR products. To confirm that both lines were knock-outs and thus, that the T-DNA insertions effectively interrupted gene transcription, total RNA was isolated from WT and mutant leaves and Reverse Transcriptase PCR (RT-PCR) was performed using gene-specific primers. Neither *ppp7a* nor *ppp7b* showed residual transcription of the respective interrupted gene (**Figure 3.8.B**). Due to the high homology between PPP7A and PPP7B and to analyze their likely

redundant function, the double mutant *ppp7ab* was created crossing homozygous *ppp7a* plants with *ppp7b* plants. The F_2 generation was then screened by PCR for homozygous double mutants.
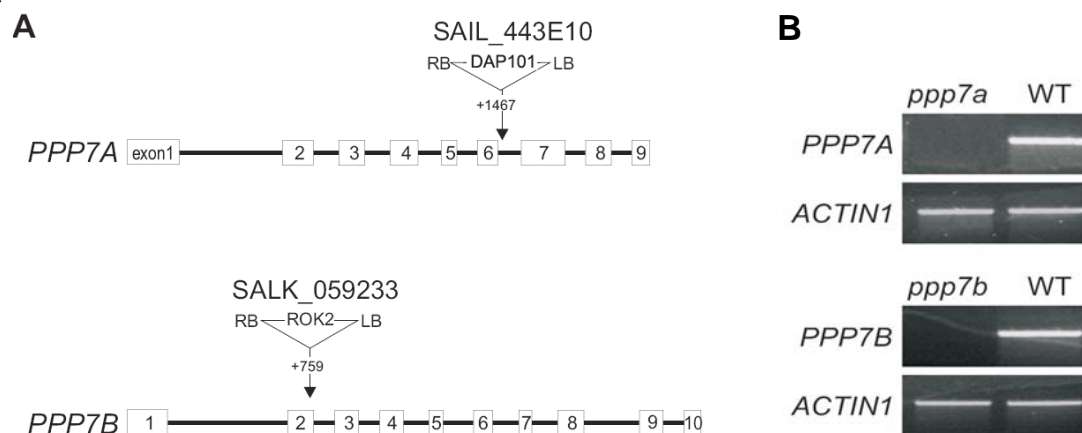
Fig 3.8. Mutations of *PPP7A* and *PPP7B* genes and their effects on transcript accumulation. **A**: The translated parts of exons (boxes), as well as intron sequences (lines) are depicted. The T-DNA insertion sites and orientation are provided and drawn not in scale. **B**: Transcript levels were detected by RT-PCR. Amplicons were selected 5' of the insertion for *ppp7a* and 3' for *ppp7b*. PCR was carried out for 40 cycles using gene- and Actin1-specific primer (the latter as a control).

To investigate the expression level of *PPP7A* and *PPP7B*, antibodies were raised against PPP7 proteins (see Material and Method). The protein level of PPP7A and PPP7B was different: in *ppp7a* mutant backgrounds PPP7B is only weakly expressed compared with the homologue PPP7A, detected in *ppp7b* single mutant. In the double mutant *ppp7ab*, PPP7 proteins are completely missing (**Figure 3.9**).
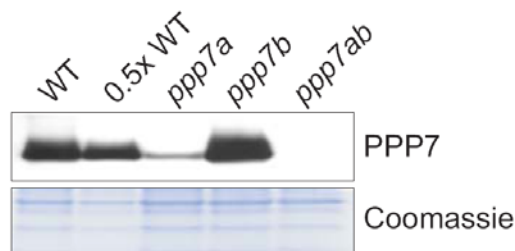
Fig 3.9. Western analysis of PPP7 content in thylakoid membrane of WT and mutant plants. Lanes were loaded with 5 μg of chlorophyll except lane 0.5xWT and probed with αPPP7 antibodies. Coomassie staining of the same gel serves as a loading control

Both, single and double mutants could germinate and grow photoautotrophycally on soil (**Figure 3.10**). Only *ppp7ab* double mutant shows a relatively pale green leaf coloration and reduced biomass under controlled greenhouse growth conditions. Chlorophyll content analysis (**Table 3.2**) showed a reduced amount of total chlorophyll while the *chl* a/b ratio was unchanged.

Fig 3.10. Growth phenotype of 3-week-old WT, *ppp7a* and *ppp7b* single mutants as well as the *ppp7ab* double mutant. Plants were grown in greenhouse under long-day conditions.

Sample	Pigments in pmol per mg fresh weight							
	VAZ	**Nx**	**Lut**	**Car**	***Chl* a**	***Chl* b**	***Chl* a+b**	***Chl* a/b**
WT	59 ± 5	83 ± 6	288 ± 24	183 ± 8	1722 ± 94	521 ± 38	2243 ± 132	3.31 ± 0.08
ppp7ab	46 ± 5	65 ± 10	217 ± 37	141 ± 18	1300 ± 187	399 ± 56	1699 ± 243	3.26 ± 0.08

Table 3.2. Pigment composition of WT and *ppp7ab* double mutant leaves. Pigment content was determined by HPLC of leaves from four different plants each genotype. Mean values ±SD are shown. VAZ: xanthophylls cycle pigments (violaxanthin + antheraxantin + zeaxanthin); Nx: Neoxanthin; Lu: Lutein; Car: β-carotene; *Chl*: chlorophyll.

3.5 <u>Complementation of the mutations</u>

Since for each gene only one line could be identified in the available mutant collections, it has been necessary to complement the phenotype of the double mutant *ppp7ab* with both genes *PPP7A* and *PPP7B*. To achieve this, the entire coding sequence of both genes has been cloned under the control of the 35SCaMV promoter and the constructs were used to transform *ppp7ab* double mutant plants. Positive transformants were selected by hygromycin resistance and the insertion was confirmed by PCR with specific primers (refer to Material and Methods for a list). The presence of PPP7 proteins was eventually detected by Western analysis (**Figure 3.11**). The complementation of the phenotype was also analyzed in terms of photosynthetic

performance confirming that under the control of the 35SCaMV promoter both genes can complement the mutation and indeed have redundant functions.
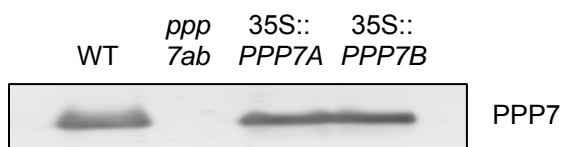
Fig 3.11. Complementation of *ppp7ab* with both *PPP7A* and *PPP7B*. All lanes are loaded with thylakoid extraction corresponding to 5 μg of chlorophyll.

3.6 The mutations do not cause any loss in the content of thylakoid proteins

PPP7 proteins are integrated into the thylakoid membrane and their loss could have deleterious effects on the organization of the photosynthetic machinery. To test this possibility, native one- and two-dimensional gels were performed using β-DM to solubilise thylakoid proteins of WT and *ppp7ab* double mutant plants. β-DM is a mild detergent known to preserve the supra-structure of complexes by isolating them from the lipid-films. One dimensional blue native gels showed that there are no differences between WT and double mutant regarding the organization of the photosynthetic machinery in super-complexes (**Figure 3.12**).
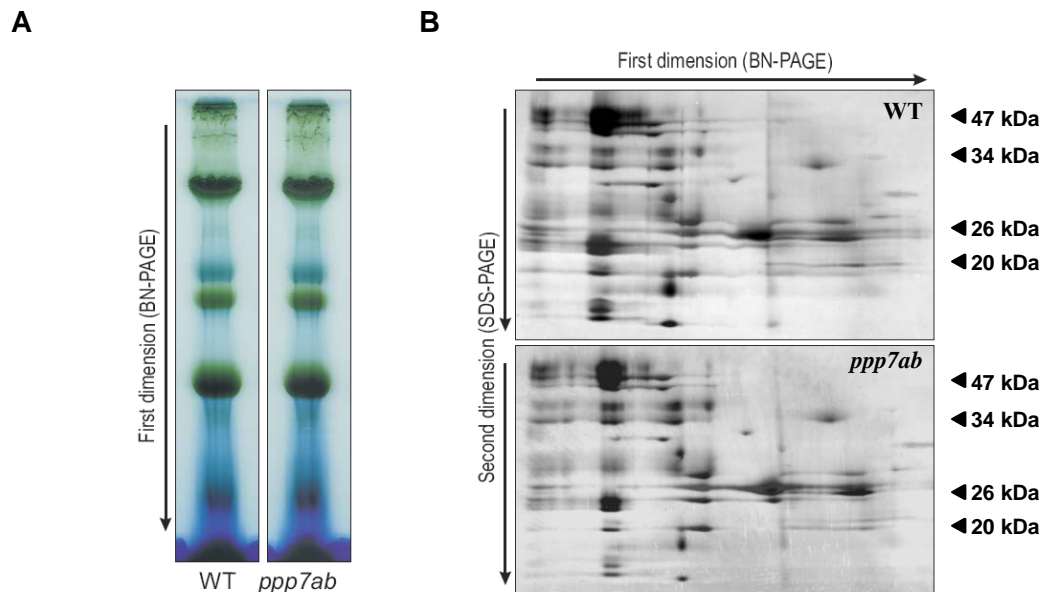
Fig 3.12. Separation of complexes and super-complexes of the photosynthetic machinery. **A**. One dimension BN-PAGE using 100 μg of chlorophyll each lane. **B**. Lanes of the first dimension BN-PAGE gel were then loaded on an SDS-PAGE acrylamide gel for the second dimension run and stained with non-quantitative silver staining.

### 3.7 <u>Mutants lacking PPP7s are impaired in photosynthesis</u>

Photosynthetic electron transport was characterized in detail by comparing the light intensity dependence of chlorophyll fluorescence parameters between mutant and WT plants using a Pulse Amplitude Modulated chlorophyll fluorometer (PAM). Both single mutants behaved indistinguishable from WT, still expressing the PPP7 protein to varying degrees because of residual expression of *PPP7* transcript from the non-mutated locus (**Figure 3.9**). In the *ppp7ab* double mutant the maximum quantum yield (F_V/F_M) is similar to WT (**Table 3.3**). The fraction of the primary electron receptor of PSII (Q_A) present in the reduced state, estimated by the parameter 1-qP, is increased in the double mutant plants. Moreover, the effective quantum yield of PSII (Φ_{II}) is reduced. Taken together, these findings suggest an unaltered electron flow through PSII, while a downstream step of the electron transfer could be affected.

In addition, under the control of the 35SCaMV promoter, both genes can restore the WT photosynthetic phenotype in the double mutant background, confirming the redundancy of their function.

| Parameter	*ppp7a*	*ppp7b*	*ppp7ab*	WT	35S::*PPP7A*	35S::*PPP7B*
F_V/F_M	0.83 ± 0.01	0.83 ± 0.01	0.83 ± 0.01	0.83 ± 0.01	0.83 ± 0.02	0.83 ± 0.01
Φ_{II}	0.76 ± 0.02	0.74 ± 0.02	0.66 ± 0.02	0.75 ± 0.01	0.74 ± 0.02	0.76 ± 0.02
1-qP	0.05 ± 0.02	0.07 ± 0.02	0.13 ± 0.02	0.06 ± 0.01	0.08 ± 0.02	0.07 ± 0.03

Table 3.3. Spectroscopic data for mutant and WT leaves. Mean values ± SD (5 plants each genotype) are shown. For the double mutants transformed with the 35S::*PPP7* constructs, the data of only one complemented line of each gene are listed.

Supporting previous results, the electron transport rate (ETR) was not affected at low light intensities in *ppp7ab* mutants (**Figure 3.13**) but remains lower than in WT at higher light intensities. Non photochemical quenching was induced with increasing light intensities but this induction was impaired in comparison to WT (**Figure 3.13**). Both of these findings resemble the behaviour of the *pgr5* mutant with a defective CEF around PSI (Munekage *et al.*, 2002). For this reason, *pgr5* has been included as an additive control in the following measurements.
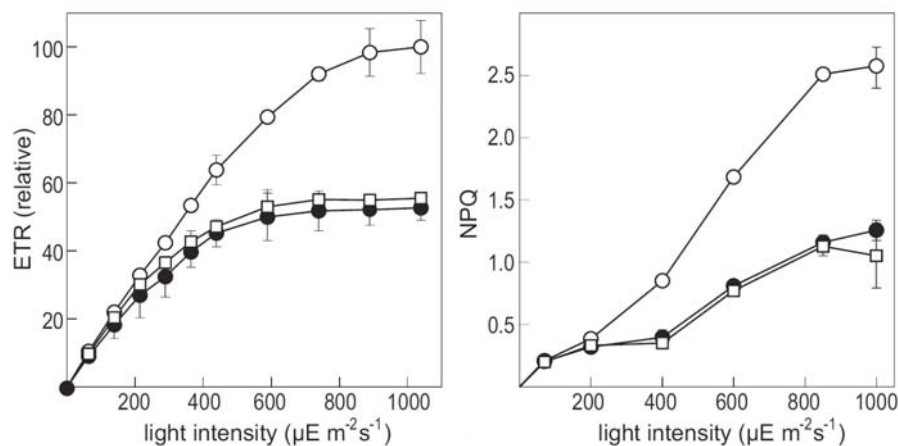
Fig 3.13. Light intensity dependence of the electron transport rate (ETR) and of non-photochemical quenching. ETR is depicted relative to the maximal value in WT; NPQ is calculated from chlorophyll fluorescence in WT and mutant leaves. White circles: WT plants; black circles: *ppp7ab*; white squares: *pgr5*. Each value represents the mean ± standard deviation (5 plants each genotype).

NPQ is measured mainly as thermal dissipation of excitation energy from PSII (qE) triggered by luminal acidification. When dark adapted leaves are exposed to light, immediate acidification of the lumen drives a rapid and transient increase of NPQ within the first minute. After further two minutes a relaxation of NPQ can be observed. This relaxation is due to the fact that the intensity of 80 $\mu E\ m^{-2}\ s^{-1}$ is not high enough to induce thermal dissipation during steady-state photosynthesis. As it was already described for the *pgr5* mutant (Munekage *et al.*, 2002), also in *ppp7ab* this transient increase in NPQ is reduced when compared with WT (**Figure 3.14**). This indicates that in both *pgr5* and *ppp7ab* the thylakoid lumen was not acidified enough to induce transient thermal dissipation.
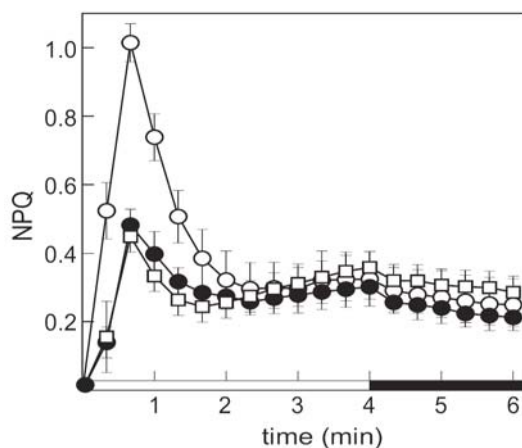
Fig 3.14. Time course of induction and relaxation of NPQ. Induction and relaxation of NPQ were monitored for 4 min at 80 $\mu E\ m^{-2}s^{-1}$ (white bar) and 2 min in the dark (black bar) on dark adapted leaves of WT plants (white circles), *ppp7ab* (black circles) and *pgr5* mutants (white squares). Each value represent the mean ± standard deviation (5 plants each genotype).

45

Considering that *pgr5* and *ppp7ab* mutants could be impaired in the same pathway, the absence of the PPP7 protein should have an effect on the oxidation ratio of the PSI reaction centre, as well as on the redox state of the plastoquinone, similar to *pgr5*.

In order to monitor the redox state of P_{700}, the changes in the difference of absorbance at 810 and 860 nm have been evaluated. P_{700} is oxidised to P_{700}^+ under different light intensities. The level of oxidation is measured as ΔA. The oxidation is followed by a reduction in the dark and re-oxidation, to a maximum level, under far-red light (measured as ΔA_{MAX}). The light dependence of the P_{700} oxidation ratio can then be calculated as $\Delta A / \Delta A_{MAX}$. In the *ppp7ab* double mutant (as in *pgr5*) the P_{700} stays in a reduced state already at relatively low light intensities (**Figure 3.15**).
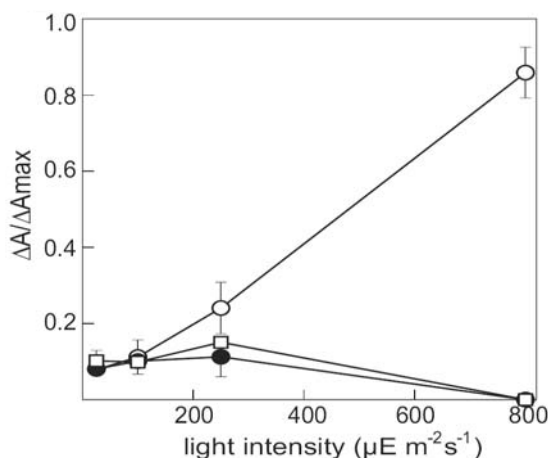

Fig 3.15. Light intensity dependence of the P_{700} oxidation ratio ($\Delta A / \Delta A_{MAX}$) in dark adapted leaves of WT plants (white circles), *ppp7ab* (black circles) and *pgr5* mutants (white squares). Each value represents the mean ± standard deviation (5 plants each genotype).

3.8 <u>Mutants lacking PPP7 are impaired in cyclic electron flow around PSI</u>

It has been shown that in *pgr5* mutant the ferredoxin-dependent plastoquinone reduction is decreased. To examine this phenotype also in *ppp7ab*, plastoquinone reduction was monitored *in vitro* as an increase in chlorophyll fluorescence. Under illumination of ruptured chloroplasts with light of low intensity (1 $\mu E\ m^{-2}\ s^{-1}$) the detectable chlorophyll fluorescence reflects the reduction of plastoquinone by cyclic electron transport from ferredoxin. In this assay, NADPH is used as an electron source via the reverse reaction of ferredoxin-NADPH reductase enzyme (Myake and Asada, 1994; Munekage *et al.*, 2002). Also mutants defective in linear electron flow were tested to determine the CEF level when linear flow is slightly impaired. This was done to clarify whether the presumable defects in CEF in *ppp7ab* and *pgr5* are just secondary effects due to an altered linear electron flow. As shown in **Figure 3.16**, in *ppp7ab* as well as in the *pgr5* mutant, the ferredoxin-dependent plastoquinone reduction is impaired indicating that

PPP7 and PGR5 operate in the same pathway associated with Fd-dependent CEF. Interestingly, under the tested conditions, linear electron flow defective *Arabidopsis* mutants *psad1-1* (Ihnatowicz *et al.*, 2004) and *psae1-3* (Ihnatowicz *et al.*, 2007) show a slightly higher reduction of the plastoquinone pool, which is already induced by the addition of the NADPH (in WT, *pgr5* and *ppp7ab*, NADPH addition do not cause any significant increase in chlorophyll fluorescence). These findings clearly suggest that impaired linear electron flow does not necessarily result in a defective cyclic electron transfer.
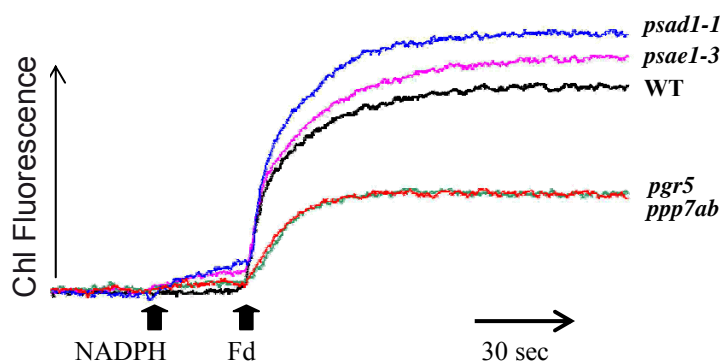
Fig 3.16. Increase of chlorophyll fluorescence by addition of NADPH (0.25 mM) and ferredoxin (Fd, 5 µM) under weak measuring light (1 µE m^{-2} s^{-1}) was monitored in osmotically ruptured chloroplasts (20 µg chlorophyll/mL) of WT, *psae1-3*, *psad1-1*, *pgr5* and *ppp7ab* mutants.

To measure the occurrence of CEF around PSI in intact leaves, another method was applied as already described (Joliot *et al.*, 2004; Joliot and Joliot, 2002; Nandha *et al.*, 2007). During these measurements the P_{700} oxidation kinetics is tracked under illumination with far-red light in a way that only PSI photochemistry is active. The slow P_{700} oxidation observed in dark-adapted leaves is supposed to represent the occurrence of CEF, whereas the fast P_{700} oxidation observed in light-adapted leaves should reflect the rate of LEF because of the activated Calvin cycle (Joliot and Joliot, 2005).

Without pre-illumination, *ppp7ab*, *pgr5* and WT plants exhibit similar P_{700} oxidation kinetics (**Figure 3.17**). In leaves that were first illuminated for 5 min with green light to activate linear electron flow, oxidation of P_{700} occurred as rapidly in *ppp7ab* plants as in the *pgr5* mutant and WT plants. These results imply that, under those conditions, LEF replaces CEF with equal efficiency in all three genotypes. However, after shorter periods of priming with green light, both *ppp7ab* and *pgr5* showed faster P_{700} oxidation than WT, clearly suggesting that the CEF-to-LEF transition occurs more rapidly in the two mutants. In the same assay, P_{700} oxidation is

suppressed in dark-adapted leaves of *psad1-1* mutants (**Figure 3.17**), indicating that they show increased rates of CEF. This is in agreement with the results obtained from the in vitro assay as depicted in **Figure 3.16**.
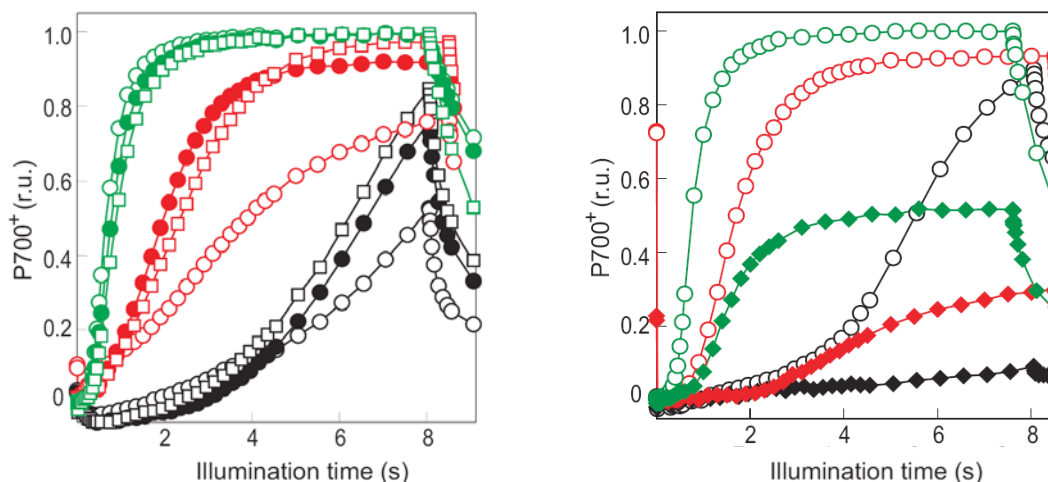

Fig 3.17. Quantification of CEF in intact leaves. P_{700} oxidation was induced by illumination with far-red light. Dark-adapted leaves from WT (open circles in the left and right panel), *ppp7ab* (filled circles, left panel), *pgr5* (squares, left panel) and *psad1-1* (filled diamonds, right panel) plants were illuminated for different time intervals with green light to induce LEF (black color: 0 s and red color: 20 s), and P_{700} oxidation was recorded 200 ms after the green light was switched off. The P_{700} oxidation after 5-min exposure to green light, followed by 2 min in the dark is indicated by green curves. The data are presented as relative values.

In conclusion the applied *in vitro* and *in vivo* assays indicate that CEF is disturbed to similar extents in both *ppp7ab* and *pgr5* mutants. However, the relative severity of the measured CEF defects differs between the two assays: the intact-leaf assay detects an imbalanced CEF-to-LEF transition and a slight reduction in the maximum rates of CEF while the *in vitro* assay suggests that the CEF capacity is markedly reduced.

Considering that *pgr5* and *ppp7ab* mutants show a defective CEF which results in a reduced capacity to induce NPQ during the dark-to-light transition, it could be concluded that increased CEF can result in a higher reduction of the plastoquinone pool.

Ultimately this stronger reduction of the plastoquinone pool could lead to an increase in the induction of transient NPQ. Indeed, this could be confirmed for the *psad1-1* and *psae1-3* mutants (**Figure 3.18**).
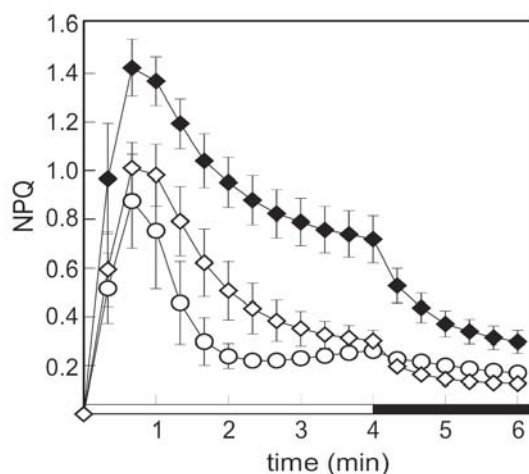
Fig 3.18. Time course of induction and relaxation of NPQ. Induction and relaxation of NPQ were monitored for 4 min at 80 µE $m^{-2}s^{-1}$ (white bar) and 2 min in the dark (black bar) on dark adapted leaves of WT plants (white circles), *psad1-1* (dark diamonds) and *psae1-3* mutants (white diamonds). Each value represents the mean ± standard deviation (5 plants each genotype).

3.9 PPP7 interacts *in vitro* with PGR5, Fd, FNR, PSI and cyt b_6/f

To identify possible interaction partners of PPP7, proteins that were shown to be involved in CEF around PSI or to mediate linear electron transfer through the stromal sides of PSI and the cyt b_6/f complexes were taken into consideration.

Since PPP7A is integrated in the thylakoid membrane, the Split Ubiquitin Assay was chosen, which has been comprehensively described in Pasch *et al*. (2005). For the interaction study, the coding sequence of mature PPP7A has been cloned in the pAMBV4 vector fused to the C terminus of the Ubiquitin gene (Cub), whereas the to be tested interactors (Fd, PSI-D, Cyt b_6, and the two leaf isoforms of FNR, FNR1 and FNR2) were cloned into the pADSL vector fused to the sequence coding for the N terminus of the Ubiquitin protein (Nub).

The yeast strain DSY-1 was co-transformed with various combinations of bait and prey plasmids (see Material and Methods) and the ability to grow on selective media was tested to confirm the success of the co-transformation (medium lacking leucine and tryptophan). The ability to grow on medium lacking leucine, tryptophan and histidine was a proof for the interaction between the two putative interactors. Negative controls were also included in the interaction assay (see Material and Methods). The interaction of PPP7A with proteins not involved in CEF was also tested. In particular, the PSII core protein D1, the integral subunit of the chloroplast ATPase CF_0-IV (both transmembrane proteins) and stromal components involved in shuttling LHC proteins from the envelope to the thylakoid membrane (cpSRP54 and 43) were chosen as preys.

According to the results of the split ubiquitin assay, PPP7A interacts with PGR5 and with the proteins involved in electron transfer (Fd and FNR) or involved in CEF (Cyt b_6 and PSI-D). There was no detectable interaction with subunits of PSII or the ATPase complex (**Table 3.4**). To investigate the interaction of PGR5 with the other PPP7 interactors, the yeast two hybrid assay was applied. The *PGR5* coding sequence corresponding to the mature protein form, was cloned in the vector pGADT7 carrying the GAL4 DNA activation domain, whereas the sequences encoding the prey proteins were cloned in the pGBKT7, carrying the GAL4 DNA binding domain.

The yeast strain AH109 was co-transformed with the indicated combinations of bait and prey plasmids and its ability to grow on selective media was tested to confirm the success of the co-transformation (medium lacking tryptophan and leucine) and the interaction between the two putative interactors (β-galactosidase activity). Negative controls were performed as described in Material and Methods.

In the yeast two hybrid assay, PGR5 was found to interact only with ferredoxin. Also the N- and the C-terminal part of PPP7A were tested via the Y2H assay for interaction with PGR5, but only weak interactions could be detected between Fd and the C-terminal part of PPP7A (**Table 3.4**). No further interactions could be detected, implying that both loops might be required for the correct folding structure necessary for such interactions.

	PGR5	FNR1	FNR2	Fd	PSI-D	Cyt b_6	PSII-D1	ATPaseIV	cpSRP
PPP7A	+[a]	+[a]	+[a]	+[a]	+[a]	+[a]	-[a]	-[a]	-[a]
PGR5	-[b]	-[b]	-[b]	+[b]	-[b]	+[a]	nd	nd	nd

Table 3.4. protein-protein interactions between PPP7 or PGR5 and other thylakoid proteins. [a] split ubiquitin assay; [b] yeast two hybrid assay. -: negative interaction; +: positive interaction; nd: not determined.

Given that the topology of PPP7 proteins allows an efficient protein-protein interaction only between the stromal exposed N- and C-terminal domains, it could be concluded that also PGR5 is localized on the stromal side of the thylakoid membrane. This stromal localisation of PGR5 was confirmed by immunoblot analysis with PGR5-specific antibodies after mild trypsin treatment of intact thylakoids (**Figure 3.19**). The abundance of negatively charged amino acids within the N-terminal loop of PPP7 (see **Figure 3.2**) suggests a possible electrostatic interaction with the positively charged PGR5 protein (Munekage *et al.*, 2002) in this region.
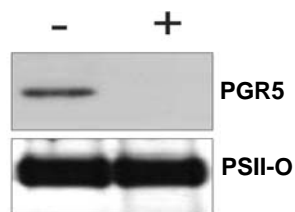
Fig 3.19. Immunoblot analysis with antisera specific for PSII-O and PGR5 proteins before (lane –) and after (lane +) trypsin treatment of intact thylakoid membranes. Lanes were loaded with thylakoids corresponding to 5 μg of chlorophyll.

3.10 PPP7 interacts *in planta* with PSI and PGR5

It has already been shown that the lack of PPP7 does not affect the organization of the photosynthetic machinery (see **Figure 3.12**). In consequence, it is of major interest to understand whether PPP7 and its interactor PGR5, are part of a specific complex or if they are only transiently associated with the cyt b_6/f complex and/or PSI. To answer this question, the presence of PPP7 and PGR5 proteins has been investigated in mutants lacking the different photosynthetic complexes: *hcf136* lacks a PSII assembly/stability factor and as a consequence, the entire PSII (Plücken *et al.*, 2002); *psad1psad2* lacks both PSI-D isoforms (Ihnatowicz *et al.*, 2004) and therefore the PSI complex is missing in this mutant. In *petc* the gene coding for the Rieske protein is not functional and the mutant lacks the entire cyt b_6/f complex (Maiwald *et al.*, 2003). Finally, *atpd* was chosen as a mutant defective in the ATPase due to a mutation in the gene coding for the ATPase δ subunit (Maiwald *et al.*, 2003). As showen in **Figure 3.20** PPP7 and PGR5 proteins are both present in all of the mutants tested. This suggests a stable integration in the thylakoid membrane independent from the known major complexes. PPP7 and PGR5 seem also not to influence the stability of the photosynthetic complexes since all the major complexes are present in the *ppp7ab* and *pgr5* mutants.
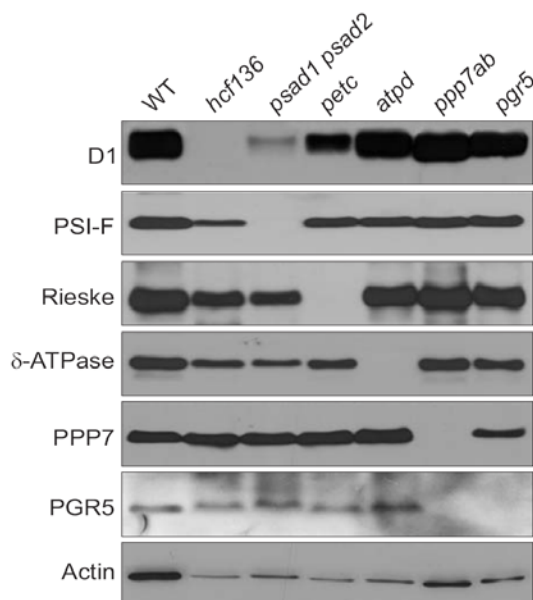
Fig 3.20. Immunodetection of the different subunits of photosynthetic complexes in WT, *hcf136*, *psad1psad2*, *petc*, *atpd*, *ppp7ab* and *pgr5* mutants. On the left the used antibodies are indicated. Lanes were loaded with total protein extracts corresponding to 10 μg of proteins.

Interestingly, is that in the absence of PPP7 no accumulation of PGR5 could be observed (**Figure 3.20**) whereas PGR5 expression is not essential for accumulation of PPP7 (in the *pgr5* mutant, PPP7 is only marginally decreased). To analyse the relationship between PPP7 and PGR5 in more detail, preparations of total chloroplasts, thylakoids and stroma fraction were probed with antibodies specific for PGR5 and PPP7 (**Figure 3.21**). It could be confirmed that in the absence of PGR5, PPP7 still accumulates in the thylakoid membrane, while no traces of PGR5 can be detected in chloroplasts of *ppp7ab* plants. The slightly reduced accumulation of PPP7 in *pgr5* plants can only be attributed to post-translational regulation (e.g. protein degradation) since on the mRNA level, the amount of transcripts of *PGR5* and *PPP7* was not altered in *ppp7ab* and *pgr5* plants (**Table 3.5**). In case of PPP7 not being present in the thylakoid membrane, PGR5 is probably synthesized but also rapidly degraded as no traces of PGR5 can be found in the stroma fraction of *ppp7ab*.
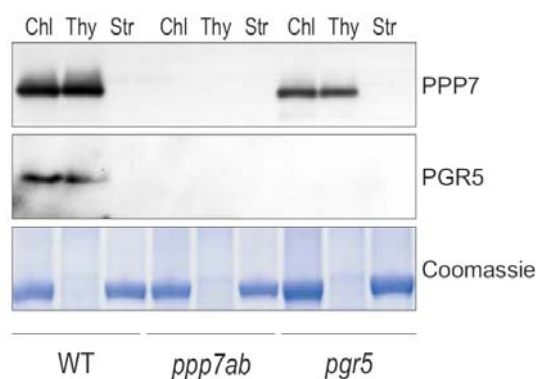

Fig. 3.21. Accumulation of PPP7 and PGR5 proteins in different chloroplast subfractions of WT, *ppp7ab* and *pgr5* plants. Lanes "chl" correspond to 5 μg chlorophyll of intact chloroplasts. Lanes "Thy" correspond to the thylakoid fraction resulting from the osmotic lysis of chloroplasts corresponding to 5 μg chlorophyll. Lanes "Str" correspond to the stromal fraction of the same lysis reaction. In the bottom panel, as control for the purity of the fractions, a Coomassie stained part of the gel is shown, where the large subunit of Rubisco migrated,

Transcript	*ppp7a*	*ppp7b*	*ppp7ab*	*pgr5*
PPP7A	0 ± 0	96 ± 8	0 ± 0	198 ± 37
PPP7B	60 ± 8	0 ± 0	0 ± 0	96 ± 13
PGR5	85 ± 35	71 ± 18	125 ± 20	$1330 \pm 799*$

Table 3.5. Real Time RT-PCR analyses on the transcript levels of *PGR5, PPP7A* and *PPP7B* in *pgr5, ppp7a, ppp7b* and *ppp7ab* mutant leaves. Values are in % of WT and *ACTIN1* transcript levels were used as an internal control. The values are calculated according to the $2^{-\Delta\Delta CT}$ method (Livak). *The *pgr5* point mutation prevents accumulation of the PGR5 protein although it also results in increased levels of *PGR5* mRNA.

Multiple factors could cause the impairment of CEF, which occurs in *ppp7ab* and *pgr5* mutants. One possibility could be that other components of the CEF machinery are defective or reduced, for example the cyt b_6/f complex or the NDH complex, which is responsible for the reduction of plastoquinone by NADPH. To answer this question, Western analyses have been carried out on thylakoid preparation of WT, *ppp7ab* and *pgr5* mutants using antibodies against subunits of both complexes. As shown in **Figure 3.22** the defect in CEF in *ppp7ab* and *pgr5* can be entirely explained by the lack of PGR5 and PPP7 proteins in these mutants, because the cyt b_6/f complex and the NDH complex are normally present in both mutant lines..
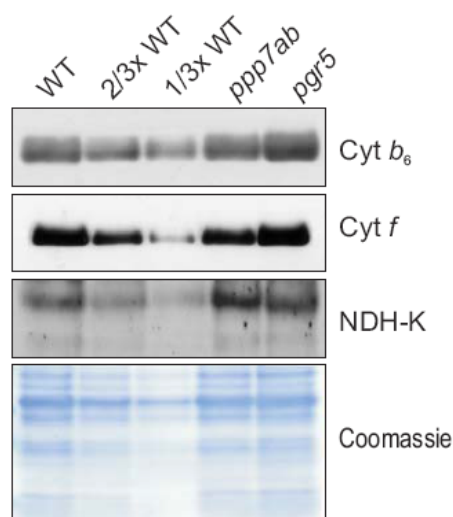
Fig. 3.22. Accumulation of subunits of the cyt b_6/f and NDH complexes in WT, *ppp7ab* and *pgr5* mutant plants, detected by Western analysis. Analyses were performed on thylakoid proteins using specific antibodies raised against Cyt b_6, Cyt f and subunit K of the plastid NDH complex. Lower amounts of WT proteins were loaded in lanes 2/3x WT and 1/3x WT, as indicated. In the bottom panel, a replicate gel stained with Coomassie Blue is shown as a loading control.

### 3.11 PPP7/PGR5-PSI interaction and PSI organization

As previously shown, PGR5 and PPP7 are involved in CEF (**Figure 3.14** and **3.16**). Still, it remains to be clarified whether they are part of the PSI complex or "only" transiently associated with it. PSI was hence isolated from *pgr5*, *ppp7ab* and WT leaves and probed with antibodies against PGR5 and PPP7. As shown in **Figure 3.23** both proteins are present in the PSI fraction. If one compares equal amounts of PSI fractions and thylakoid extraction, it can be concluded that PPP7 is less abundant in PSI.

With PGR5 this does not seem to be the case. In other words, the interaction of PPP7 with PGR5 is not necessary for the stability of PPP7 (see also **Figure 3.21**); rather PPP7 requires PGR5 to stably interact with PSI. It could also be possible that a fraction of PPP7 present in the thylakoid membrane, does not bind PGR5.
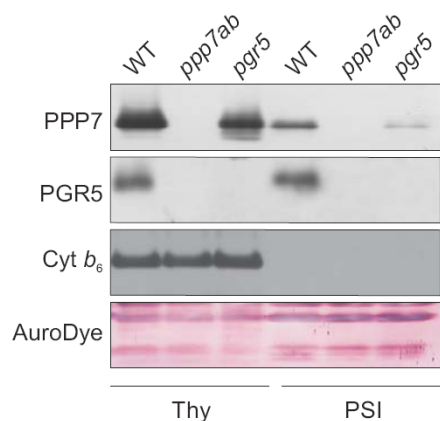
Fig 3.23. Immunodetection of PGR5 and PPP7 in thylakoids and PSI fractions of WT and mutant leaves. Thylakoids were loaded equal to 3.5μg of chlorophyll, while the PSI fractions were loaded corresponding to 5 μg of chlorophyll. The lower panel shows the AuroDye (GE Healthcare) staining of the membrane after blotting, to confirm equal loading.

Because PGR5 and PPP7 are associated with the PSI complex and *ppp7ab* is defective in linear electron flow, it was important to figure out whether the lack of PGR5 and PPP7 is affecting the composition or structure of PSI and therefore influencing the linear electron flow. For that, PSI has been isolated from *pgr5, ppp7ab* and WT leaves via sucrose gradient followed by SDS-PAGE using 16 to 23% gradient gels. The analyses revealed that absence of PGR5 or PPP7 does not influence the composition of PSI (**Figure 3.24**) supporting the idea that these proteins are not subunits of PSI.
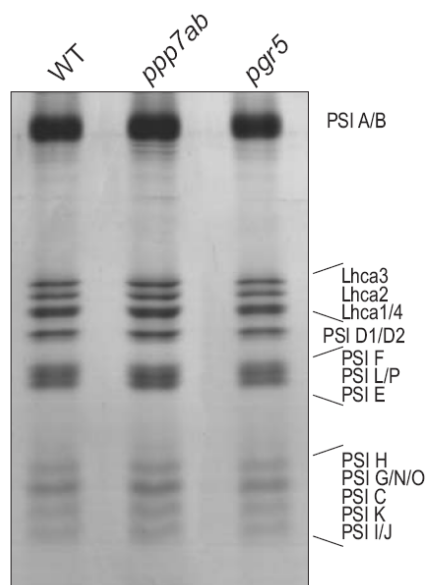
Fig 3.24. PSI subunit composition in wild-type and mutant plants. Equal amounts (corresponding to 5 μg of chlorophyll) of PSI isolated from mutant and WT leaves were fractionated by SDS-PAGE on a 16 to 23% acrylamide gel and visualised by Colloidal Coomassie staining. The positions of subunits were previously identified by immunodetection (Jensen *et al.*, 2002)

3.12 CEF and abundance of Fd, FNR, PPP7 and PGR5

The data reported in **Figure 3.16** and **3.17** show that CEF is altered in the *ppp7ab* double mutant, as well as in *psae1-3* and *psad1-1* mutants. To clarify whether the components of CEF at the stromal side of PSI (Fd, FNR) and in the thylakoid membrane (PPP7 and PGR5) are changed in their abundance in mutants with decreased (*pgr5* and *ppp7ab*) or increased (*psae1-3* and *psad1-1*) CEF efficiency, Western analyses have been carried out with thylakoid extractions of WT, *ppp7ab*, *pgr5*, *psad1-1* and *psae1-3* mutants. As it can be seen in **Figure 3.25**, the Fd content associated to the thylakoid membrane is significantly increased in *psad1-1* and *psae1-3*, whereas FNR is equally present in all analysed genotypes. A slight increase in the PPP7 and PGR5 protein content can be observed for the mutants defective in linear electron flow. Since there are no difference in the Fd accumulation between the PSI fractions of *psae1-3* and *psad1-1* compared to WT (**Figure 3.25**), it can be concluded that the excess of Fd could be bound to the cyt b_6/f complex or some other complex in the thylakoid membrane.
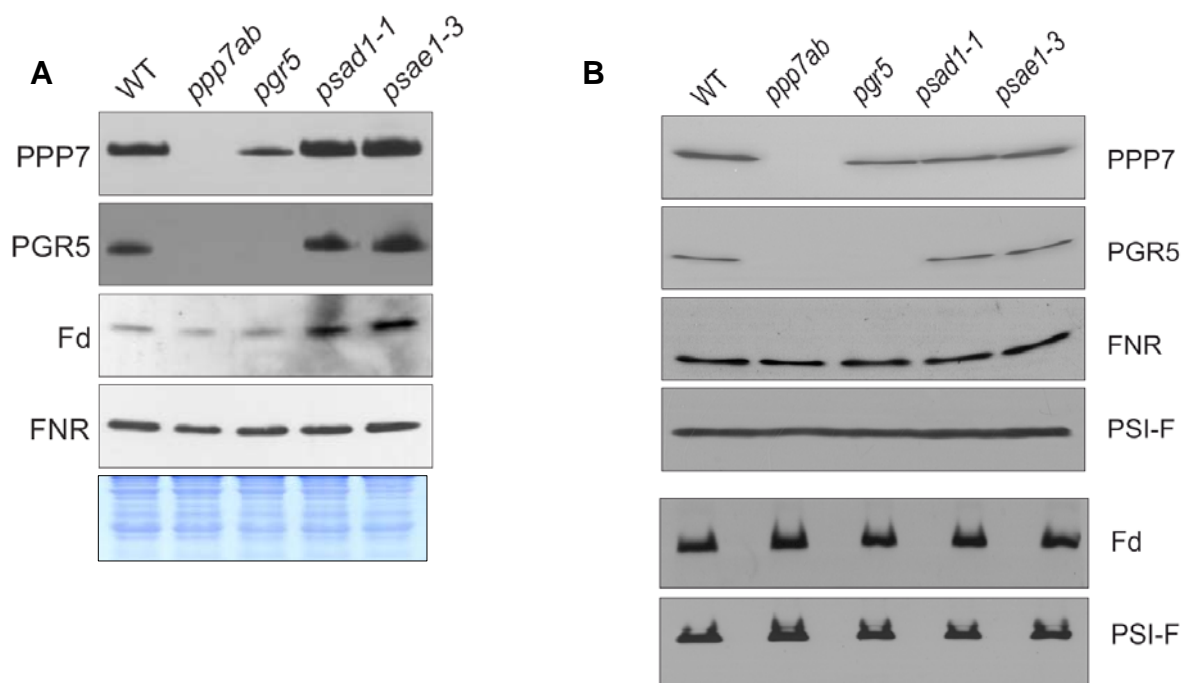

Fig 3.25. Western analyses of the CEF machinery. **A:** All lanes were loaded with thylakoid extractions corresponding to 5 µg of chlorophyll. Different antibodies (listed on the side) were used to quantify the protein contents in WT, *ppp7ab*, *pgr5*, *psad1-1* and *psae1-3* mutant plants. A replica gel was stained with Coomassie Blue as a loading control (bottom panel). In panel **B**, all lanes were loaded with PSI fractions corresponding to 5 µg of chlorophyll. The membrane tested with Fd antibodies was loaded with protein amounts corresponding to 10 µg of chlorophyll. PSI-F antibodies were used in both filters as a control for equal loading.

3.13 Synthetic phenotype of the *ppp7ab psad1-1* triple mutant

From the previous results, it can be suggested that in mutants with a defective linear electron flow, the CEF is enhanced. This might lead to an increased acidification of the lumen and consequent NPQ induction. Indeed, opposite to the *pgr5* and *ppp7ab* mutants, the *psad1-1* and *psae1-3* mutants show a faster transient induction of NPQ upon dark to light transition. Because PPP7 appears to be present in large excess in WT plants (in *ppp7a* single mutant, PPP7b level of only 10% is sufficient to maintain WT phenotype, see **Figure 3.10** and **3.11**) the slight increase of PPP7 and PGR5 protein levels in *psae1-3* and *psad1-1* could be responsible for the increase in CEF. If this is the case, severe effects on plant performance should be detectable in a triple mutant defective in PSI-D or PSI-E and PPP7. For this purpose *ppp7ab psad1-1* triple mutants were generated by crossing *psad1-1* single mutant with and *ppp7ab* double mutants. The segregating F2 progeny was screened for homozygous triple mutants via PCR. The lack of PPP7 and PGR5 was confirmed by Western analysis.

As shown in **Figure 3.26**, the triple mutant is significantly decreased in its growth (compared to *psad1-1*) and has a pale green coloration.
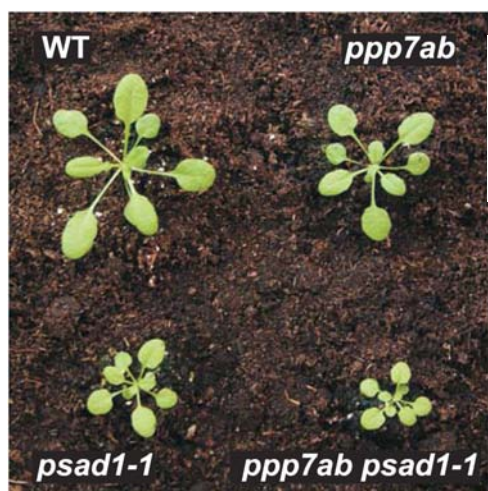
Fig 3.26. Growth phenotypes of 3-week-old WT, *ppp7ab, psad1-1* and *ppp7ab psad1-1* mutants. Plants were grown in the greenhouse under long-day conditions.

The transient increase in non-photochemical quenching, which can be observed in *psad1-1* during the transition from dark-to-light, occurs also in the triple mutant *ppp7ab psad1-1* though less prominent than in the *psad1-1* single mutant (**Figure 3.27**). Surprisingly, the *ppp7ab* mutation is not inhibiting the NPQ phenotype of *psad1-1* in the triple mutant and this could be explained by an involvement of PPP7 in the regulation of CEF rather than PPP7 being a direct component of CEF itself. Another explanation could be that the remaining NDH is

compensating the deficiency in the PPP7/PGR5 depending pathway even though its efficiency is decreased.
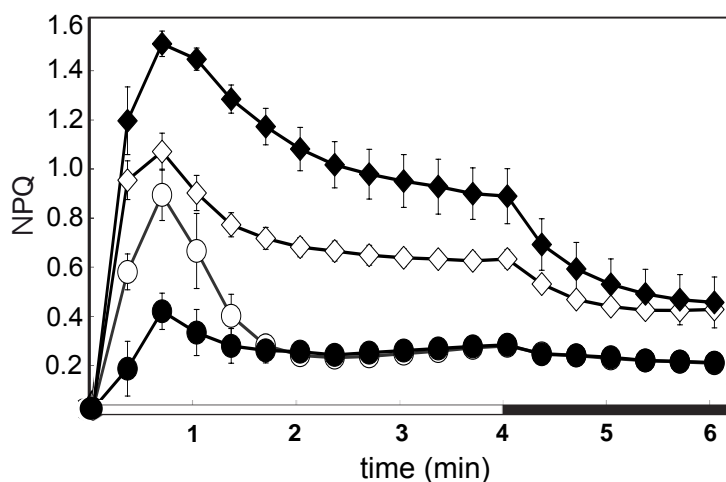
Fig 3.27. Time course of induction and relaxation of NPQ. Induction and relaxation of NPQ were monitored for 4 min at 80 µE m^{-2}s^{-1} (white bar) followed by 2 min in the dark (black bar) using dark adapted leaves of WT plants (white circles), *psad1-1* (dark diamonds), *ppp7ab psad1-1* (white diamonds) and *ppp7ab* mutants (dark circles). Each value represent means ± standard deviation (5 plants each genotype).

Analysing the CEF activity in the triple mutants, chlorophyll measurements on *in vitro* ruptured chloroplasts showed that *ppp7ab psad1-1* triple mutants perform CEF at a similar extent as *ppp7ab* mutant (**Figure 3.28)**.
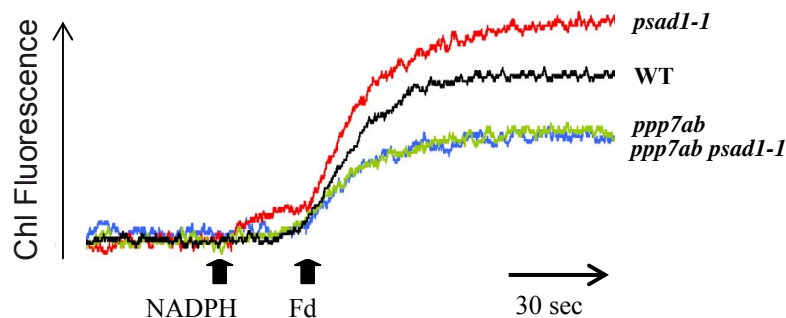
Fig 3.28. Increases of chlorophyll fluorescence by addition of NADPH (0.25 mM) and Ferredoxin (Fd, 5 µM) under the illumination of weak measuring light (1 µE m^{-2} s^{-1}) was monitored in osmotically ruptured chloroplasts (20 µg chlorophyll/mL) of WT, *psad1-1, ppp7ab* and *ppp7ab psad1-1* mutants.

As it was demonstrated for *ppp7ab*, also in the case of the triple mutant the measurement of CEF via the *in vivo* analysis provides different result. As can be seen in **Figure 3.29**, the *in vivo* estimation of the CEF suggests that even considering the significantly lower signal, the

triple mutant *ppp7ab psad1-1* has an intermediate activity in comparison with the two parental mutants.
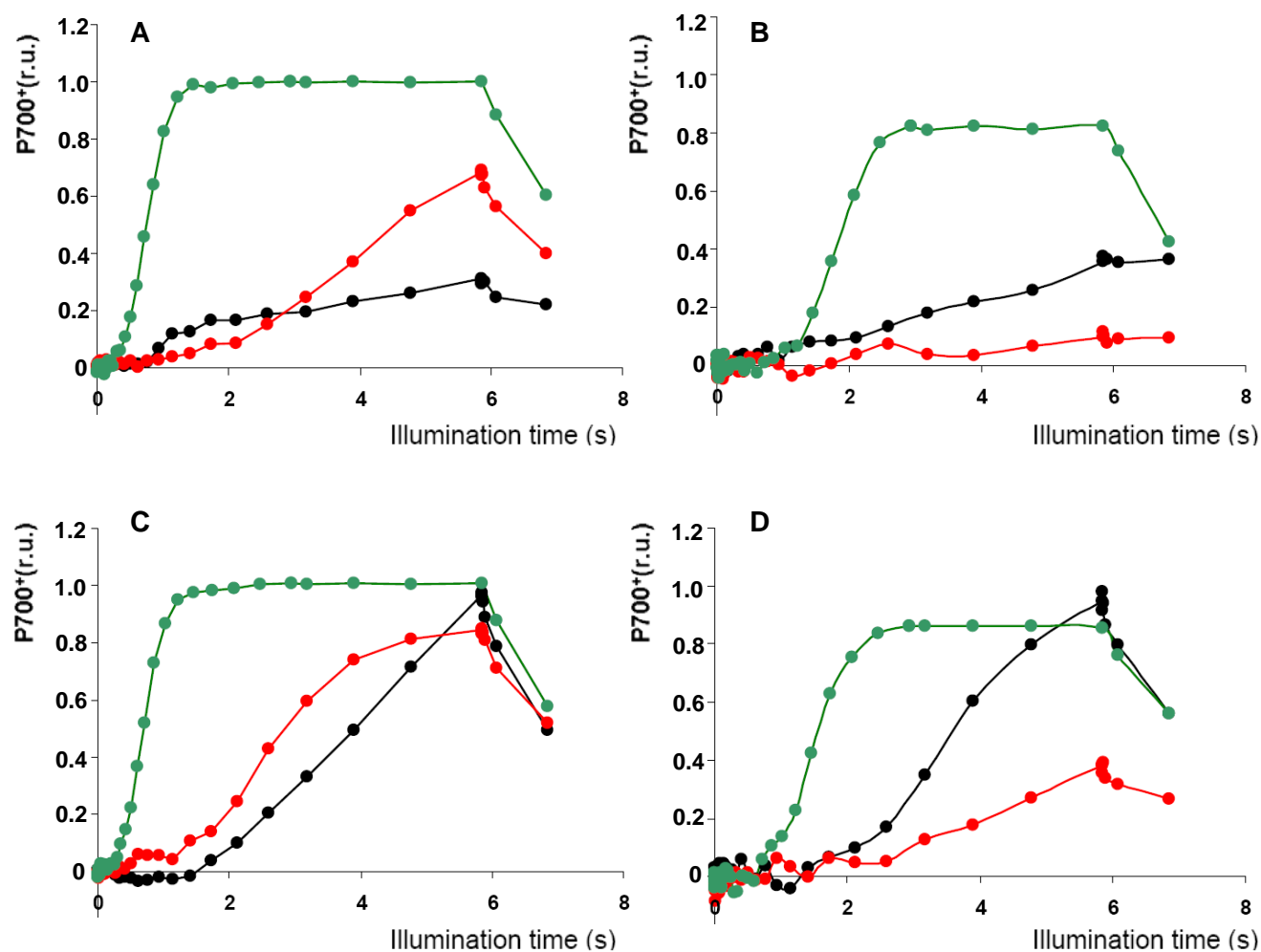
Fig 3.29. Quantification of CEF in intact leaves. P_{700} oxidation was induced by illumination with far-red light. Dark-adapted leaves from WT (panel **A**), *psad1-1* (panel **B**), *ppp7ab* (panel **C**) and *ppp7ab psad1-1* (panel **D**) plants were illuminated for different times with green light to induce LEF (black colour 0 s and red colour 20 s), and P_{700} oxidation was recorded 200 ms after the green light was switched off. A 10-min exposure to green light, followed by 2 min in the dark is indicated by green curves. Data are expressed as relative values.

4. Discussion

4.1 <u>PPP7: a novel component of CEF around PSI</u>

Since the discovery of cyclic electron flow (CEF), the pathway(s) taken by the electrons to flow around PSI remain unclear and under debate. The existence of at least two possible routes, via ferredoxin (Fd) and via the plastidial NADPH dehydrogenase (NDH), is generally accepted but their interconnections and interactions are still obscure.

Recently the protein PGR5 has been identified as a component of the antimycin-A sensitive Fd-dependent pathway and the effects of a lack of PGR5 in chloroplasts have been subject of extensive studies (Munekage *et al.*, 2002; Munekage *et al.*, 2004). The phenotype of the *pgr5* mutant in *Arabidopsis* suggests that PGR5 plays either a direct role in CEF (Shikanai, 2007) or acts as a regulator of the switch between linear and cyclic electron transfer (Avenson *et al.*, 2005; Nandha *et al.*, 2007) with its absence leading to a reduced capability of CEF to compete with linear electron flow. To date, the exact function of PGR5 and its precise localization in the thylakoid membrane are still unclear.

This thesis focuses on an *Arabidopsis* protein that we named PPP7, a novel component of the thylakoid machinery involved in the electron transfer from ferredoxin to plastoquinone.

Orthologous genes coding for PPP7 proteins can be found in the genomes of higher plants and eukaryotic algae (**Figure 3.2**) as well as mosses. Apparently it is not encoded by the genome of cyanobacteria, leading to the conclusion that it is an eukaryotic invention.

The genome of *Arabidopsis thaliana* contains two genes (*At4g22890* and *At4g11960*) coding for homologous proteins with redundant functions, PPP7A and PPP7B. PPP7A is highly expressed, while PPP7B is only weakly expressed. The mRNA of both genes can be found in green tissues but not in roots (**Figure 3.1**). The proteins are targeted to the chloroplasts where they fold into the thylakoid membranes in a manner that the N- and C-terminal domains are exposed towards the stroma (**Figure 3.3, 3.4 and 3.6**).

Our data suggest that due to this topology, PPP7 interacts with PGR5 which is present on the stromal side (**Figure 3.19**). Supporting this model, PGR5 has been characterized to be associated with, but not integrated into, the thylakoid membrane because it does not contain any transmembrane domain (Munekage *et al.*, 2002). In the *Arabidopsis* double mutant *ppp7ab*, completely devoid of PPP7, the *PGR5* gene is normally transcribed but probably the

protein is not able to anchor on the membrane via PPP7 and therefore it is most likely rapidly degraded. On the other hand, if PGR5 is missing, PPP7 is still synthesized and integrated into the thylakoid membrane but to a lesser extent (**Figure 3.20**).

The interaction of the PPP7/PGR5 complex with other proteins in the thylakoid membrane is still not clear. It seems to be transiently but not tightly associated with PSI (**Figure 3.20**) or cytb_6/f (**Table 3.4**). The PPP7/PGR5 complex is not a structural component of the major photosynthetic complexes and most likely it is present and stable by itself in the thylakoid membrane (**Figure 3.20**). Confirming these hypotheses, the depletion of PPP7 and consequently of PGR5 does not affect the organization and composition of the photosynthetic machinery and mutant plants can grow photo-autotrophically (**Figure 3.10** and **3.12**).

4.2 PPP7 and PGR5 proteins are involved in the same pathway of CEF

Regarding photosynthetic performance, PPP7 and PGR5 functionally interact and can be considered as components or, at least, regulators of the ferredoxin-dependent CEF around PSI.

In *ppp7ab* plants, the reaction centre of the PSI (P_{700}) remains in a reduced state during actinic light illumination and it is oxidized to a normal level only under far red light, which favours mainly PSI photochemistry (**Figure 3.15**). This phenotype may be explained by the phenomenon called charge recombination in P_{700}, which is caused by an over-reduction of the stromal electron acceptors from PSI, ferredoxin and $NADP^+$. Under these conditions, electrons return to P_{700} from the PSI-acceptor-side electron carriers (i.e. A_0, A_1, F_X and F_A/F_B). This has been proven by the fact that the artificial electron acceptor methylviologen, known to acquire electrons directly from the early acceptors of PSI, is restoring WT P_{700} oxidation ratio in the *pgr5* mutant (Munekage *et al.*, 2002). The results obtained with the methylviologen treatment provide an indication that this limited P_{700} oxidation is not due to a defect in the electron transfer chain within PSI. Moreover, taking into account that treating isolated thylakoids of *pgr5* with exogenous electron acceptors, linear electron flow (LEF) appears to occur as in WT plants (Munekage *et al.*, 2002) and it can be concluded that the linear electron flow is not *per se* impaired in *pgr5* and therefore, most likely also not in *ppp7ab*.

Hence, the over-reduction of the electron carriers on the stromal side of PSI could be explained by a defective CEF around the PSI.

Up to now there are two techniques that are thought to directly quantify CEF. The first, developed by Shikanai and co-workers (Endo *et al.*, 1998), is an *in vitro* evaluation of the electron transfer from the ferredoxin to the plastoquinone pool. In this assay, exogenous ferredoxin is used as electron carrier and the NADPH as electron source. NADPH donates electrons indirectly via reduced ferredoxin generated by the thylakoid-bound ferredoxin NADP$^+$ reductase (FNR). In this assay only the first steps of CEF are monitored, but the destiny of the electrons, once loaded on the plastoquinone, is not followed. Applying this assay, the *ppp7ab* mutant and the *pgr5* mutant show a markedly reduced CEF (**Figure 3.16**).

On the other hand, the *in vivo* measurements of CEF designed by Joliot and Joliot (2006) are estimating the rate of the oxidation of PSI. In this way, only the oxidation rate of P$_{700}$ is considered, independently where the electrons go or come from. By this method, *ppp7ab* and *pgr5* mutants result to be impaired only in the transition between cyclic and linear electron flow, while they both potentially perform WT level of CEF (**Figure 3.17**).

It is not easy to clarify which of the two techniques is correct or most effective in measuring CEF. The differences between the two experiments are responsible for the diverse results obtained analysing the mutants. One possible conclusion, which is taking into account the result of both experiments, is that the lack of PPP7 and PGR5 results in a defective regulation of CEF around PSI. In any case, the redox state of the stroma is unbalanced in *ppp7ab* with an over-accumulation of reduced electron carriers (mostly Fd and NADPH).

Due to the reduced availability of oxidized ferredoxin, electrons are leaving PSI less rapidly and could be therefore responsible for charge recombination. Caused by this impairment of CEF in *ppp7ab* mutant, like in *pgr5*, less protons are pumped into the thylakoid lumen and as a consequence, the rapid and transient increase in non-photochemical quenching normally associated to the dark-light transition is decreased (**Figure 3.14**).

Under high light conditions this effect is even more severe, leading to a reduction of NPQ to almost 60%. This reduction of non-photochemical quenching is not responsible for those defects in linear electron flow like the decreased electron transport rate and the decreased PSII quantum yield (**Figure 3.13** and **Table 3.3**). Indeed, the linear electron transport is only marginally impaired in mutants completely lacking NPQ, as it is the case for the *Arabidopsis npq4* mutant (Li *et al.*, 2000).

Because CEF is thought to enhance ATP synthesis balancing the ATP/NADPH ratio, in *ppp7ab* the deficient ATP production could lead to an over-reduction of the stroma because of the slower consumption of reducing power in the carbon fixing reactions. This could ultimately turn in a reduced linear electron flow, reflected by a slow-growth phenotype (Avenson *et al.*, 2005; Kramer *et al.*, 2004).

4.3 A new model for CEF around PSI

To clarify the localization of the PPP7/PGR5 complex, interaction assays have been developed studying the interaction of both PPP7 and PGR5 with different subunits of the photosynthetic machinery, belonging to the PSII, PSI, cyt b_6/f complex and the ATP-synthase. Combining split ubiquitin- and yeast two hybrids-assays it has been found that the PPP7/PGR5 complex probably interacts with some of the proteins that play a role in CEF: the Fd/FNR stromal system, at least one subunit of the cyt b_6/f complex and of PSI (**Table 3.4**). In addition, a further biochemical indication is the co-purification of PPP7/PGR5 complex with PSI (**Figure 3.23**).

As already discussed, PPP7 is a membrane integrated thylakoid protein and this feature allows lateral migration and/or interaction with other multi-protein complexes. Considering these findings together, a model could be proposed for the function of the PPP7/PGR5 complex in the thylakoid membranes. In the following pictures, the possible localization of the PPP7/PGR5 complex within the thylakoid membrane and its activity are depicted.
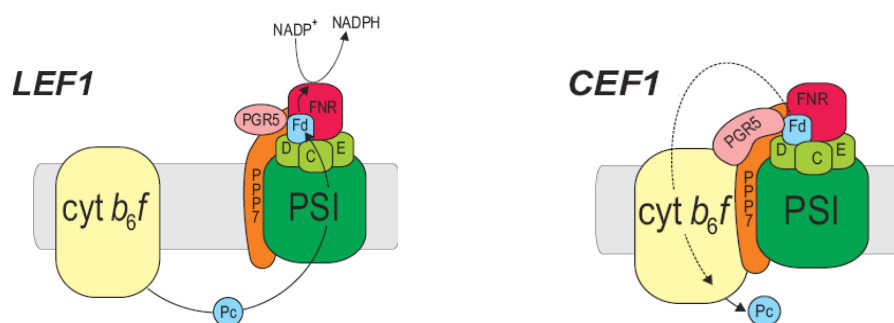
As a first thought, proven by the fact that PGR5 and PPP7 co-purify with the PSI complex (**Figure 3.23**), the complex could be imagined as tightly associated with PSI (**LEF1**) implying that during CEF the cyt b_6/f complex is in close contact with PSI and PPP7/PGR5 (**CEF1**).

Considering that both PPP7 and PGR5 can accumulate to WT levels in mutants depleted of PSI or cyt b_6/f (**Figure 3.20**) and that until now the existence of a PSI- cyt b_6/f super-complex could not be experimentally confirmed (Breyton *et al.*, 2006) this first model has to be revised.

More likely, the stability of the PPP7/PGR5 complex in the absence of PSI or cyt b_6/f suggests that during linear electron flow the PPP7/PGR5 complex is independent and free to migrate in the thylakoid membrane (**LEF2**) and it can interact alternatively with PSI and cyt b_6/f possibly shuttling FNR-Fd or creating an alternative CEF-favouring conformation (**CEF2**). This hypothesis is compatible with previous findings of FNR association with cyt b_6/f (Zhang *et al.*, 2001).
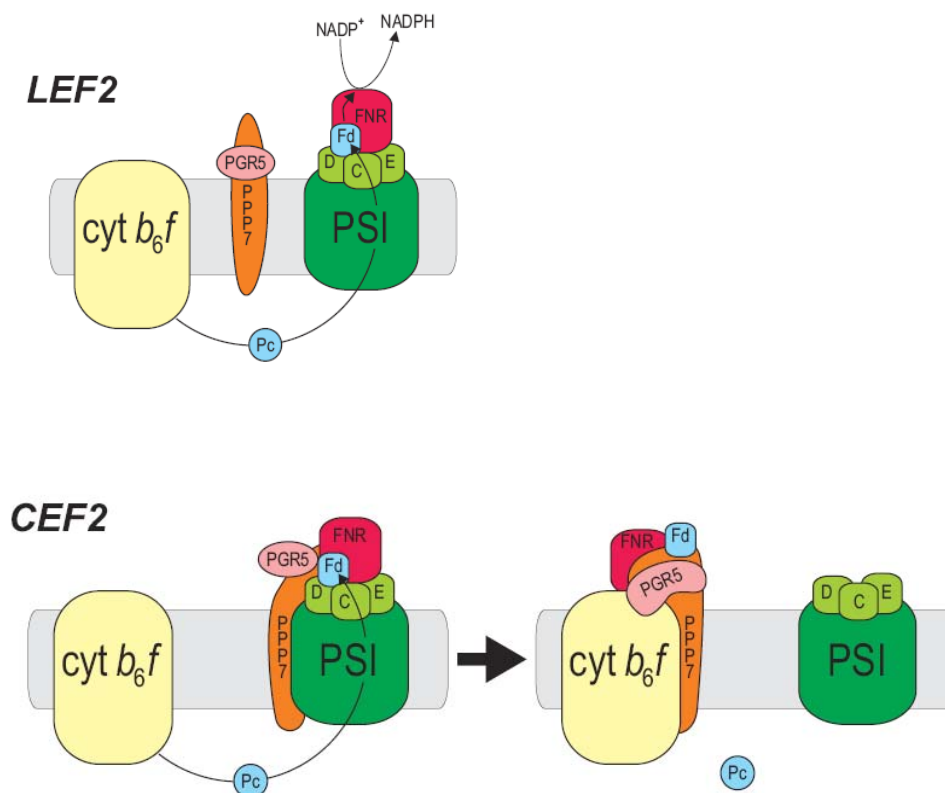
Once that FNR and Fd are bound to the PPP7/PGR5 complex and interact with the cyt b_6/f complex, the electrons could be directly injected into the plastoquinone pool without binding to any other protein (**CEF2a**) or more likely, by means of the still unidentified FQR enzyme (**CEF2b**).

63
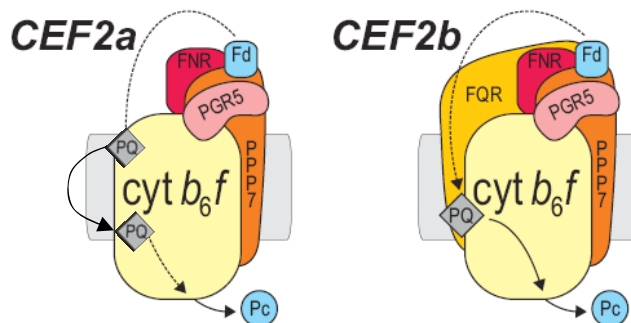
Regarding the physical way taken by electrons to reach the oxidized plastoquinone two points have to be taken into account:

- on one hand PGR5 apparently lacks known domains appointed to bind electron carrier elements (i.e. metal binding motifs or NAD^+ or FAD^+ co-enzymes) on the other hand, the biochemical properties of PPP7 are still unknown;

- the involvement of a putative FQR could not be excluded, even if the conformational arrangement offered to the Fd and FNR by binding with the PPP7/PGR5 complex could be sufficient for electron transfer.

The question is still unsolved whether the electrons are transferred directly to the oxidized forms of the plastoquinone or if auxiliary elements are involved. One of these could be represented by the novel haem (c_i) on the stromal side at the Q_i site of the cyt b_6/f complex which is a typical feature of the plastidic cytochrome complex (Kurisu *et al.*, 2003 and Stroebel *et al.*, 2003) but the actual involvement of this group in transferring electrons is still under debate. The discovery that the *pgr1* mutation (point mutation of the Rieske protein), which causes a defective Q-cycle (Okegawa *et al.*, 2005), does not affect Fd-dependent CEF, might suggest that ferredoxin directly donates electrons to oxidized plastoquinone (PQ) and not to the cyt b_6/f complex. Alternatively, it is also possible that the *pgr1* mutation does not affect electron transport from Fd to PQ through the cyt b_6/f complex. In this last case, PGR5 together with PPP7 could be factors facilitating the access of Fd to the cyt b_6/f complex.

4.4 Cyanobacteria do not have PPP7

PPP7 does not have homologues in cyanobacteria. This could be puzzling at first sight, since the PGR5 protein is conserved among these species. It has to be taken into account that cyanobacterial cyt b_6/f preparations lack the FNR, in contrast to plant preparation (Zhang *et al.*,

2001). This indicates that the formation of the complex depicted in **CEF2** model could be a specific feature of eukaryotic thylakoids, implying that cyanobacteria developed slightly different pathways and regulatory mechanisms of cyclic flow around PSI. Supporting this hypothesis is that in *Synechococcus* sp. PCC7002 the PSI subunit E is required for CEF *in vivo* (Yu *et al.*, 1993) and in fact mutants lacking this subunit show defective CEF.

In vascular plants, PSI-E is not essential for CEF and moreover, the *A. thaliana psae1-3* mutant seems to perform even higher CEF around PSI (**Figure 3.16** and **3.17**). Probably PSI-E is involved in the binding during the formation of an hypothetical "cyclic flow super-complex" and therefore its lack results in a less stable or malfunctioning complex.

It appears possible that in cyanobacteria, PGR5 alone is sufficient to stabilize an interaction between PSI (or Fd) and cyt b_6/f or the complex responsible for the electron transfer from ferredoxin to plastoquinone. Furthermore, differently from the eukaryotic ferredoxin, the cyanobacterial one has a short C-terminal helix extending from the vicinity of its Fe-S cluster (Fukuyama *et al.*, 1980). It might be considered that this carboxy-terminal helix could penetrate into the cyt b_6/f complex binding to the haem c_i (Cramer *et al.*, 2006). Also in this case, PGR5 alone could be responsible for the protein rearrangement appointed to switch from linear to cyclic flow.

4.5 <u>Independent accumulation of PPP7 from PGR5</u>

Regarding the stoichiometry between PPP7 and PGR5 it is interesting to notice that probably not the entire pool of PPP7 found in the thylakoid membrane is bound to PGR5. As showed in **Figure 3.23**, the ratio PPP7 to PGR5 in the thylakoid membranes is lower than the ratio between the two proteins bound to the PSI. It is reasonable that PPP7 is explicating more than one function in the thylakoid membranes. Unfortunately, until now all transgenic lines carrying *PPP7A* or *PPP7B* genes under control of the 35S promoter failed in over-expressing PPP7 and therefore a direct control of the effect of over-expression of PPP7 is still missing. On the other hand the over-expression of PGR5 resulted in plants with defective chloroplast development (Okegawa *et al.*, 2007). Moreover, the stromal redox state is unbalanced by the over-accumulation of PGR5.

It is well documented that ferredoxin and $NADP^+/NADPH$ play a crucial role as redox regulator in the chloroplasts. These molecules are involved in regulating enzymes of the Calvin

cycle via the thioredoxin system and as electron source for nitrogen and sulphur metabolism and the general plastidic anabolism. Therefore, fine adjustment of the amount of reduced ferredoxin and of the $NADP^+/NADPH$ ratio needs to be rigorously controlled. In this way the abundance of PGR5 and PPP7 could be an important factor adjusting the competition between linear and CEF, according to the environmental conditions and specific requirements of reducing powers or electrons donors.

4.6 <u>Link between LEF and CEF</u>

The discussion about the cause-effect relationship between impaired CEF and decreased LEF is still open. Our data support the idea that a defect in CEF results in a defective LEF, but the opposite seems not to be the case. It has been extensively reported that *Arabidopsis* mutants *psad1-1* and *psae1-3* display a reduced linear electron flow (Varotto *et al.*, 2000; Ihantowicz *et al.*, 2004; Ihnatowicz *et al.*, 2007). Interestingly they seem to have increased CEF (**Figure 3.16** and **3.17**), a fact that is confirmed by the higher NPQ induction during the dark-to-light transition (**Figure 3.18**). This can be explained if we assume that a reduced content of PSI-E or PSI-D leads to a decreased amount of FNR that transfer electrons from Fd to $NADP^+$. Under these circumstances, an alternative route could be followed by electrons that leave PSI to be promptly re-injected into the plastoquinone pool.

In accordance with this hypothesis, *psad1-1* and *psae1-3* show a higher amount of thylakoid-bound Fd, PPP7 and PGR5 (**Figure 3.25**). Interestingly, a closer look of **Figure 3.16** shows that the addition of NADPH to *psad1-1* and *psae1-3* ruptured chloroplasts induces a slight increase in chlorophyll fluorescence, which is not found in WT and in the other analysed genotypes. This could be explained when considering that the amount of ferredoxin bound to the thylakoid membranes in *psad1-1* and *psae1-3* is higher than in WT. It seems plausible that this higher level of endogenous ferredoxin is responsible for the electron transfer from NADPH to the reduced plastoquinone pool. In the case of WT and *ppp7ab* (as well as *pgr5*) the smaller amount of ferredoxin bound to the thylakoids could result in a negligible increase in chlorophyll fluorescence.

An alternative explanation of the higher CEF displayed by *psad1-1* and *psae1-3* could be that under genetic conditions limiting the transfer of electrons from Fd to $NADP^+$, CEF is activated

as protection mechanism, dissipating excessive energy of the active PSII through increased luminal acidification that turns in induction of NPQ.

Since the amount of required PPP7 is probably relatively low (considering that roughly just 10% of the protein is enough to give WT phenotype, see **Figure 3.9** and **3.10**) the increase in the level of the PPP7/PGR5 complex in *psae1-3* and *psad1-1* mutants could be sufficient for the increase in CEF. Interestingly, when both linear electron flow and this safety valve are shut down (as in the triple mutant *ppp7ab psad1-1*), the plant is still able to survive even if decreased in size and paler in leaf coloration (**Figure 3.26**).

Regarding the activity of CEF, preliminary results based on the *in vitro* techniques show that CEF activity in the *ppp7ab psad1-1* triple mutant is comparable to that of the *ppp7ab* mutant (**Figure 3.28**). On the other hand, if CEF is measured according to the *in vivo* measurement developed by Joliot and colleagues, *ppp7ab psad1-1* appears to have an intermediate phenotype between *ppp7ab* and *psad1-1* (**Figure 3.29**). In any case, it is important to notice that the lack of the PPP7/PGR5 complex cause a defective CEF even in a mutant that is genetically prompt to higher cyclic activity.

As a consequence, the transient NPQ normally generated during the dark-to-light transition is decreased. Noticeably, as showed in **Figure 3.27,** the NPQ of the triple mutant is reduced if compared to *psad1-1*, but remains higher than in WT leaves. A possible explanation for this phenotype could be represented by the alternative cyclic pathways through the NDH complex. This alternative route probably compensates the defective ferredoxin-dependent pathway even though it is supposed to be less efficient (Sazanov *et al.*, 1998; Joet *et al.*, 2002).

Alternatively, we could consider that PPP7 and PGR5 are rather involved in the switch between linear to CEF, rather than in CEF itself. In this case, the *psad1-1* genetic background favourites cyclic flow upon linear. In the triple mutant, the lack of the PPP7/PGR5 complex denies the possibility for the enhanced switch from linear to cyclic. As a result, the depletion of one of those mechanisms enabling plants to cope with the fluctuating environmental conditions is ultimately influencing the plant fitness.

4.7 <u>CEF and state transition</u>

The trigger of the switch between linear electron flow and CEF is another issue that needs to be discussed when comparing green algae to vascular plants. It has been first hypothesised and then demonstrated in *Chlamydomonas* that CEF is activated upon induction of state transition (Finazzi and Forti, 2004).

LHCII migration along the thylakoids is responsible for a membrane rearrangement in the chloroplast (Georgakopulos and Argyroudi-Akoyunoglu, 1994). During state transition some grana lamellae disassemble and convert into stroma lamellae. Due to his membranes reorganization, the accessibility of the cyt b_6/f to the PPP7/PGR5 complex binding Fd-FNR could be higher, increasing the ferredoxin pool that contributes to cyclic flow (Finazzi and Forti, 2004). It has been shown that when the cells switch from state 1 to state 2 the electron flow pathway switches from linear to cyclic (Finazzi *et al.*, 1999).

A rationale for this switch could be the fact that when PSI is equipped with LHCII and its activity increases, it could be necessary to generate a secure electron source to compensate the PSII reduced activity. On the other hand, if PSI is more active, the risk of reduction of molecular oxygen is higher. Under these conditions, a safety system that re-directs electrons to the plastoquinone pool preventing oxygen reduction would support photosynthetic flexibility.

Whether this mechanism would appreciably modify photosynthetic electron flow in higher plants is still unknown. The population of LHCII antennae that move from PSII to PSI during the state transition is highly different considering algae and higher plants. While in the first species around 80% of the total antennae complex goes under state transition, in higher plants only 20% of the LHCII population is thought to migrate to PSI (Allen, 1992; Delosome *et al.*, 1996). Concerning this aspect, the availability of mutants defective in state transition as well as mutants with increased or decreased CEF, will definitely stimulate further research understanding the regulation of the mechanisms responsible for the adjustment of chloroplast's redox state.

5. References

- Albertsson P.A. (2001) A quantitative model of the domain structure of the photosynthetic membrane. *Trends Plant Sci* 6: 349-354

- Allakhverdiev S.I., Nishiyama Y., Miyairi S., Yamamoto H., Inagaki N., Kanesaki Y. and Murata, N. (2002) Salt stress inhibits the repair of photodamaged photosystem II by suppressing the transcription and translation of *psbA* genes in *Synechocystis*. *Plant Physiol* 130: 1443-1453

- AllenJ. F. (1992) Protein phosphorylation in regulation of photosynthesis. *Biochim Biophys Acta* 1098: 275-335

- Allen J. F. and Forsberg J. (2001) Molecular recognition in thylakoid structure and function. *Trends Plant Sci* 6: 317-326

- Alonso J.M., Stepanova A.N., Leisse T.J., Kim C.J., Chen H., Shinn P., Stevenson D.K., Zimmerman J., Barajas P., Cheuk R., Gadrinab C., Heller C., Jeske A., Koesema E., Meyers C.C., Parker H., Prednis L., Ansari Y., Choy N., Deen H., Geralt M., Hazari N., Hom E., Karnes M., Mulholland C., Ndubaku R., Schmidt I., Guzman P., Aguilar-Henonin L., Schmid M., Weigel D., Carter D.E., Marchand T., Risseeuw E., Brogden D., Zeko A., Crosby W.L., Berry C.C., Ecker J.R. (2003) Genome-wide insertional mutagenesis of *Arabidopsis thaliana*. *Science* 301: 653-657

- Arnon D.I., Whatley F.R. and Allen M.B. (1955) Vitamin K as a cofactor of photosynthetic phosphorylation. *Biochim Biophys Acta* 16: 607-608

- Aronsson H. and Jarvis P. (2002) A simple method for isolating import-competent *Arabidopsis* chloroplasts. *FEBS Letters* 529: 215-220

- Bassi R., dal Belin Peruffo A., Barbato R. and Ghisi R. (1985) Differences in chlorophyll-protein complexes and composition of polypeptides between thylakoids from bundle sheaths and mesophyll cells in maize. *Eur J Biochem* 146: 589-595

- Bassi R., Marquardt J. and Lavergne J. (1995) Biochemical and functional properties of photosystem II in agranal membranes from maize mesophyll and bundle sheath chloroplasts. *Eur J Biochem* 233: 709-719

- Bendall D.S. and Manasse R.S. (1995) Cyclic photophosphorilation and electron transport. *Biochim Biophys Acta* 1229: 23-38

- Berman-Frank I., Lundgren P. and Falkowski P. (2003) Nitrogen fixation and photosynthetic oxygen evolution in cyanobacteria. *Res Microbiol* 154: 157-164

- Biehl A., Richly E., Noutsos C., Salamini F. and Leister D. (2005) Analysis of 101 nuclear transcriptomes reveals 23 distinct regulons and their relationship to metabolism, chromosomal gene distribution and co-ordination of nuclear and plastid gene expression. *Gene* 3: 33-41

- Boardman N. K. and Anderson Jan M. (1967) Fractionation of the photochemical systems of photosynthesis. II. Cytochrome and carotenoid contents of particles isolated from spinach chloroplasts *Biochim Biophys Acta* 143: 187-203

- Breyton C., Nandha B., Johnson GN., Joliot P. and Finazzi G. (2006) Redox modulation of cyclic electron flow around photosystem I in C3 plants. *Biochemistry* 45: 13465-13475

- Bukhov N. and Carpentier R. (2004) Alternative photosystem I-driven electron transport routes: mechanisms and functions. *Photosynth Res* 82: 17-33

- Bukhov N., Egorova E. and Carpentier R. (2002) Electron flow to photosystem I from stromal reductants in vivo: the size of the pool of stromal reductants controls the rate of

electron donation to both rapidly and slowly reducing photosystem I units. *Planta* 215: 812-820

- Burrows P.A., Sazanov L.A., Svab Z., Maliga P. and Nixon PJ. (1998) Identification of a functional respiratory complex in chloroplasts through analysis of tobacco mutants containing disrupted plastid ndh genes. *EMBO Journal* 17: 868-876

- Campbell W.J. and Ogren W.L. (1992) Light activation of Rubisco by Rubisco activase and thylakoid membranes. *Plant Cell Physiol* 33: 751-756

- Clough S. J. and Bent A. F. (1998) Floral dip: a simplified method for *Agrobacterium*-mediated transformation of *Arabidopsis thaliana*. *Plant J* 16: 735-743

- Cooley J. W., Howitt C. A. and Vermans W. F. F. (2002) Succinate quinol oxidoreductases in the cyanobacterium *Synechocystis* sp. strain PCC 6803: presence and function in metabolism and electron transport. *J Bacteriol* 182: 714-722

- Crafts-Brandner S.J. and Salvucci M.E. (2000) Rubisco activase constrains the photosynthetic potential of leaves at high temperature and CO_2. *PNAS-USA* 97: 13430-13435

- Cramer W.A., Zhang H., Yan J., Kurisu G. and Smith J.L. (2006) Transmembrane traffic in the cytochrome b6f complex. *Annu Rev Biochem* 75: 769-790

- Delosome R., Olive J. and Wollman F. A. (1996) Changes in light energy distribution upon state transition: an *in vivo* photoacoustic study of the wild type and photosynthesis mutants from *Chlamydomonas reinhardtii*. *Biochim Biophys Acta* 1273: 150-158

- Dovzhenko A., Dal Bosco C., Meurer J. and Koop H. U. (2003) Efficient regeneration from cotyledon protoplasts in *Arabidopsis thaliana*. *Protoplasma* 222: 107-111

- Endo T., Shikanai T., Takabayashi A., Asada K. and Sato F. (1999) The role of chloroplastic NAD(P)H dehydrogenase in photoprotection. *FEBS Letters* 457: 5-8

- Endo T., Shikanai T., Sato F. and Asada K. (1998) NAD(P)H Dehydrogenase-Dependent, antimycin A-sensitive electron donation to plastoquinone in tobacco chloroplasts. *Plant Cell Physiol 39*: 1226-1231

- Ernst A., Böhme H. and Böger P. (1983) Phosphorylation and nitrogenase activity in isolated heterocysts from *Anabaena variabilis. Biochim Biophys Acta* 723: 83-90

- Färber A., Young A. J., Ruban A. V., Horton P. and Jahns P. (1997): Dynamics of xanthophyll-cycle activity in different antenna subcomplexes in the photosynthetic membranes of higher plants - The relationship between zeaxanthin conversion and nonphotochemical fluorescence quenching. *Plant Physiol* 115: 1609-1618

- Finazzi G., Furia A., Barbagallo R.P. and Forti G. (1999) State transition, cyclic and linear electron transport and photophosphorylation in *Chlamydomonas reinhardtii. Biochim Biophys Acta* 1413: 117-129

- Finazzi G. and Forti G. (2004) Metabolic flexibility of the green alga *Chlamydomonas reinhardtii* as revealed by the link between state transition and cyclic electron flow. *Photosynth Res* 82: 327-338

- Friso G., Giacomelli L., Ytterberg A.J., Peltier J.B., Rudella A., Sun Q. and Wijk K.J. (2004) In-depth analysis of the thylakoid membrane proteome of *Arabidopsis thaliana* chloroplasts: new proteins, new functions, and a plastid proteome database. *Plant Cell* 16: 478-499

- Fukuyama K., Hase T., Matsumoto S., Tsukihara T., Katsube Y., Tanaka N., Kakudo M., Wada K. and Matsubara H. (1980) Structure of *Spirulina platensis* [2Fe-2S] ferredoxin and evolution of chloroplast-type ferredoxins. *Nature* 286: 522-524

- Georgakopoulos J.H. and Argyroudi-Akoyunoglou J.H. (1994) On the question of lateral migration of LHC II upon thylakoid protein phosphorylation in isolated pea chloroplasts: the stroma lamellar fraction separated from phosphorylated chloroplasts is not homogeneous. *Biochim Biophys Acta* 1188: 380-390

- Golding A.J. and Johnson G.N. (2004) Down-regulation of linear and activation of cyclic electron transport during drought. *Planta* 218: 107-114 Erratum in: *Planta.* 218: 682

- Harbinson J. and Woodward F.I. (1987) The use of light induced absorbency changes at 820 nm to monitor the oxidation state of P_{700} in leaves. *Plant Cell Environ* 10: 131-140

- Harper J.W., Adami G.R., Wie N., Keyomarsi K. and Elledge S.J. (1993) The p21 Cdk-interacting protein Cip1 is a potent inhibitor of G1 cyclin-dependent kinases. *Cell* 75: 805-816

- Havaux M., Rumeau D. and Ducruet J.M. (2005) Probing the FQR and NDH activities involved in cyclic electron transport around photosystem I by the 'afterglow' luminescence. *Biochim Biophys Acta* 1709: 203-213

- Heber U. and Walker D. (1992) Concerning a dual function of coupled cyclic electron transport in leaves. *Plant Physiol* 100: 1621-1626

- Herbert S.K., Fork D.C. and Malkin S. (1990) Photoacoustic measurements *in vivo* of energy storage by cyclic electron flow in algae and higher plants. *Plant Physiol* 94: 926-934

- Hualing M., Endo T., Ogawa T. and Asada K. (1995) Thylakoid membrane-bound, NADPH-specific pyridine nucleotide dehydrogenase complex mediates cyclic electron transport in the cyanobacterium *Synechocystis* sp. PCC 6803. *Plant Cell Physiol* 36: 661-668

- Ihnatovicz A., Pesaresi P. and Leister D. (2007) The E subunit of photosystem I is not essential for linear electron flow and photoautotrophic growth in *Arabidopsis thaliana. Planta* 226: 889-895

- Ihnatowicz A., Pesaresi P., Varotto C., Richly E., Schneider A., Jahns P., Salamini F. and Leister D. (2004) Mutants of photosystem I subunit D of *Arabidopsis thaliana*: effects on photosynthesis, photosystem I stability and expression of nuclear genes for chloroplast functions. *Plant J* 37: 839-852

- Ivanov B., Asada K. and Edwards G.E. (2007) Analysis of donors of electrons to photosystem I and cyclic electron flow by redox kinetics of P_{700} in chloroplasts of isolated bundle sheath strands of maize. *Photosynth Res* 92: 65-74

- Jach G., Binot E., Frings S., Luxa K. and Schell J. (2001) Use of red fluorescent protein from *Discosoma* sp. (dsRED) as a reporter for plant gene expression. *Plant J* 28: 483-491

- James P., Hallada, J. and Craig E. A. (1996) Genomic libraries and a host strain designed for highly efficient two-hybrid selection in yeast. *Genetics* 144: 1425-1436

- Jensen P.E., Bassi R., Boekema E.J., Dekker J.P., Jansson S., Leister D., Robinson C. and Scheller H.V. (2007) Structure, function and regulation of plant photosystem I. *Biochim Biophys Acta* 1767: 335-352

- Jensen P.E., Gilpin M., Knoetzel J. and Scheller H.V. (2000) The PSI-K subunit of photosystem I is involved in the interaction between light-harvesting complex I and the photosystem I reaction centre core. *J Biol Chem* 275: 24701-24708

- Joet T., Cournac L., Peltier G. and Havaux M. (2002) Cyclic electron flow around photosystem I in C_3 plants. *In vivo* control by the redox state of chloroplasts and involvement of the NADH-dehydrogenase complex. *Plant Physiol* 128: 760-769

- Johnson G. (2005) Cyclic electron transport in C_3 plants: fact or artefact? *J Exp Bot* 56: 407-416

- Joliot P. and Joliot A. (2002) Cyclic electron transfer in plant leaf. *PNAS-USA* 99: 10209-10214

- Joliot P., Beal D. and Joliot A. (2004) Cyclic electron flow under saturating excitation of dark-adapted *Arabidopsis* leaves. *Biochim Biophys Acta* 1656: 166-176

- Joliot P. and Joliot A. (2005) Quantification of cyclic and linear flows in plants. *PNAS-USA* 102: 4913-4918

- Kanesaki Y., Suzuki I., Allakhverdiev S.I., Mikami K. and Murata N. (2002) Salt stress and hyperosmotic stress regulate the expression of different sets of genes in *Synechocystis* sp.PCC 6803. *Biochemical and Biophysical Research Community* 290: 339-348

- Kleffmann T., Russenberger D., von Zychlinski A., Christopher W., Sjolander K., Gruissem W. and Baginsky S. (2004) The *Arabidopsis thaliana* chloroplast proteome reveals pathway abundance and novel protein functions. *Curr Biol* 14: 354-362

- Kofer W., Koop H.-U., Wanner G. and Steinmüller K. (1998) Mutagenesis of the genes encoding subunits A, C, H, I, J and K of the plastid NAD(P)H-plastoquinone-oxidoreductase in tobacco by polyethylene glycol-mediated plastome transformation. *Mol Gen Genet* 258: 166-173

- Koop H. U., Steinmüller K., Wagner H., Rößler C., Eibl C. and Sacher L. (1996) Integration of foreign sequences into the tobacco plastome via polyethylene glycol-mediated protoplast transformation. *Planta* 199: 193-201

- Kramer D. M., Avenson T. J. and Edwards G. E. (2004) Dynamic flexibility in the light reactions of photosynthesis governed by both electron and proton transfer reactions. *Trends Plant Sci* 9: 349-357

- Kurisu G., Zhang H., Smith J.L. and Cramer W.A. (2003) Structure of the cytochrome b_6/f complex of oxygenic photosynthesis: tuning the cavity. *Science* 302: 1009-1014

- Laisk A., Eichelmann H., Oja V. and Peterson R. B. (2005) Control of cytochrome b_6/f at low and high light intensity and cyclic electron transport in leaves. *Biochim Biophys Acta* 1708: 79-90

- Liu Y.G., Mitsukawa N., Oosumi T. and Whittier R.F. (1995) Efficient isolation and mapping of *Arabidopsis thaliana* T-DNA insert junctions by thermal asymmetric interlaced PCR. *Plant J* 3: 457-463

- Maiwald D., Dietzmann A., Jahns P., Pesaresi P., Joliot P., Joliot A., Levin J.Z., Salamini F. and Leister D. (2003) Knock-out of the genes coding for the Rieske protein and the ATP-synthase delta-subunit of *Arabidopsis*. Effects on photosynthesis, thylakoid protein composition, and nuclear chloroplast gene expression. *Plant Physiol* 133: 191-202

- Malkin S. and Canaani O. (1994) The use and characteristics of the photoacoustic method in the study of photosynthesis. *Annu Rev Plant Phys* 45: 493-526

- Matthijs H.C.P., Jeanjean R., Yeremenko N., Huisman J., Joset F. and Hellingwerf K.J. (2002) Hypothesis: versatile function of ferredoxin-NADP$^+$ reductase in cyanobacteria provides regulation for transient photosystem I-driven cyclic electron flow. *Funct Plant Biol* 29: 201–210

- Mi H., Endo T., Schreiber U. and Asada K. (1992) Donation of electrons from cytosolic components to the intersystem chain in the cyanobacterium *Synechococcus* sp. 7002 as determined by the reduction of P700$^+$. *Plant Cell Physiol* 33: 1099-1105

- Mills J. D., Crowther D., Slovacek RE., Hind G. and McCarty R.E. (1979) Electron transport pathways in spinach chloroplasts. Reduction of the primary acceptor of photosystem II by

reduced nicotinamide adenine dinucleotide phosphate in the dark. *Biochim Biophys acta* 547: 127-137

- Miyake C., Horiguchi S., Makino A., Shinzaki Y., Yamamoto H. and Tomizawa K. (2005) Effects of light intensity on cyclic electron flow around PSI and its relationship to non-photochemical quenching of Chl fluorescence in tobacco leaves. *Plant Cell Physiol* 46: 1819-1830

- Müller P., Li X-P. and Niyogi K.K. (2001) Non photochemical quenching. A response to excess light energy. *Plant Physiol* 125: 1558-1566

- Munekage Y., Hojo M., Meurer J., Endo T., Tasaka M. and Shikanai T. (2002) PGR5 is involved in cyclic electron flow around photosystem I and is essential for photoprotection in *Arabidopsis. Cell* 110: 361-371

- Munekage Y., Hashimoto M., Miyake M., Tomizawa K I., Endo T., Tasaka M. and Shikanai T. (2004) Cyclic electron flow around photosystem I is essential for photosynthesis. *Nature* 429: 579-582

- Munekage Y. and Shikanai T. (2005) Cyclic electron transport through photosystem I. *Plant Biotech* 22: 361-369

- Nada A. and Soll J. (2004) Inner envelope protein 32 is imported into chloroplasts by a novel pathway. *J Cell Sci* 117: 3975-3982

- Nandha B., Finazzi G., Joliot P., Haid S. and Johnson G. (2007) The role of PGR5 in the redox poising of photosynthetic electron transport. *Biochim Biophys Acta* 1767:1252-1259

- Ogawa T. and Asada K. (1994) NAD(P)H dehydrogenase-dependent cyclic electron flow around photosystem I in the cyanobacterium *Synechocystis* PCC 6803: a study of dark-starved cells and spheroplasts. *Plant Cell Physiol* 35: 163-173

- Okegawa Y., Tsuyama M., Kobayashi Y. and Shikanai T. (2005) The *pgr1* mutation in the Rieske subunit of the cytochrome *b₆/f* complex does not affect PGR5-dependent cyclic electron transport around photosystem I. *J Biol Chem* 280: 28332-28336

- Okegawa Y., Long T.A., Iwano M., Takayama S., Kobayashi Y., Covert S.F. and Shikanai T. (2007) Balanced PGR5 level is required for chloroplast development and optimum operation of cyclic electron flow around photosystem I. *Plant Cell Physiol* in press

- Osmond C.B. (1981) Photorespiration and photoinhibition: Some implications for the energetics of photosynthesis. *Biochim Biophys Acta* 639: 77-98

- Pasch J. C., Nickelsen J. and Schünemann D. (2005) The yeast split-ubiquitin system to study chloroplast membrane protein interactions. *Appl Microbiol Biot* 69: 440-447

- Peltier J.B., Emanuelsson O., Kalume D.E., Ytterberg J., Friso G., Rudella A., Liberles D.A., Soderberg L., Roepstorff P., von Heijne G. and van Wijk K.J. (2002) Central functions of the lumenal and peripheral thylakoid proteome of *Arabidopsis* determined by experimentation and genome-wide prediction. *Plant Cell* 14: 211-236

- Pesaresi P., Lunde C., Jahns P., Tarantino D., Meurer J., Varotto C., Hirtz R.D., Soave C., Scheller H.V., Salamini F. and Leister D. (2002) A stable LHCII-PSI aggregate and suppression of photosynthetic state transitions in the *psae1-1* mutant of *Arabidopsis thaliana*. *Planta* 215: 940-948

- Plücken H., Müller B., Grohmann D., Westhoff P. and Eichacker L.A. (2002) The HCF136 protein is essential for assembly of the photosystem II reaction center in *Arabidopsis thaliana*. *FEBS Letters* 532: 85-90

- Porra R. J. (2002) The chequered history of the development and use of simultaneous equations for the accurate determination of chlorophylls a and b. *Photosynth Res* 73: 149-156

- Richely E., Dietzmann A., Biehl A., Kurth J., Laloi C., Apel K., Slamini F. and Lesiter D. (2003) Covariations in the nuclear chloroplast transcriptome reveal a regulatory master-switch. *EMBO Rep* 4: 491-498

- Romanowska E., Drozak A., Pokorska B., Shiell B.J. and Michalski W.P. (2006) Organization and activity of photosystems in the mesophyll and bundle sheath chloroplasts of maize. *J Plant Physiol* 163: 607-618

- Rumeau D., Bécuwe-Linka N., Beyly A., Louwagie M., Garin J. and Peltier G. (2005) New subunits NDH-M, -N, and -O, encoded by nuclear genes, are essential for plastid Ndh complex functioning in higher plants. *Plant Cell* 17: 219-232

- Sambrook J., Fritsch E. F. and Maniatis T. (1989) *Molecular cloning*. New York: Cold Spring Harbor Laboratory Press

- Schagger H. and von Jagow G. (1987) Tricine-sodium dodecyl sulfate-polyacrylamide gel electrophoresis for the separation of proteins in the range from 1 to 100 kDa. *Anal Biochem* 166: 368-379

- Schägger H. and von Jagow G. (1991) Blue native electrophoresis for isolation of membrane protein complexes in enzymatically active form. *Anal Biochem* 199: 223-231

- Scheller H.V., Jensen P.E., Haldrup A., Lunde C. and Knoetzel J. (2001) Role of subunits in eukaryotic Photosystem I. *Biochim Biophys Acta* 1507: 41-60

- Scherer S. (1990) Do photosynthetic and respiratory electron transport chains share redox proteins? *Trens Biochem Sci* 15: 458-462

- Schreiber U., Schliwa U. and Bilger W. (1986) Continuous recording of photochemical chlorophyll fluorescence quenching with a new type of modulation fluorometer. *Photosynth Res* 10: 51-62

- Schreiber U., Klughammer C. and Neubauer C. (1988) Measuring P_{700} absorbance changes around 830 nm with a new type of pulse modulation system. *Z. Naturforsch*. 43c: 686-698

- Seidel-Guyenot W., Schwabe C. and Büchel C. (1996) Kinetic and functional characterization of a membrane-bound NAD(P)H dehydrogenase located in the chloroplasts of *Pleurochloris meiringensis* (Xanthophyceae). *Photosynth Res* 49: 183-193

- Semenova G.A. (2001) Effect of urea and distilled water on the structure of the thylakoid system. *J Plant Physiol* 158: 1041-1050

- Sherman F. (1991) Getting started with yeast. *Method Enzymol* 194: 3-21

- Shikanai T. (2007) Cyclic electron transport around Photosystem I: genetic approaches. *Annu Rev Plant Biol* 58: 199-217

- Shikanai T., Endo T., Hashimoto T., Yamada Y., Asada K. and Yokota A. (1998) Directed disruption of the tobacco ndhB gene impairs cyclic electron flow around photosystem I. *PNAS-USA* 95: 9705-9709

- Shikanai T., Munekage Y., Shimizu K., Endo T. and Hashimoto T. (1999) Identification and characterization of *Arabidopsis* mutants with reduced quenching of chlorophyll fluorescence. *Plant Cell Physiol* 40: 1134-1142

- Stroebel D., Choquet Y., Popot J.L. and Picot D. (2003) An atypical haem in the cytochrome b(6)f complex. *Nature* 426: 413-418

- Svab Z. and Maliga O. (1993) High-frequency plastid transformation in tobacco by selection for a chimeric *aadA* gene. *PNAS-USA* 90: 913-17

- Avenson T. J., Cruz J. A., Kanazawa A. and Kramer D. M. (2005) Regulating the proton budget of higher plant photosynthesis. *PNAS-USA* 102: 9709-9713

- Tagawa K., Tsujimoto H.Y. and Arnon D.I. (1963) Role of chloroplast ferredoxin in the energy conversion process of photosynthesis. *PNAS-USA* 49: 567-572

- Taiz L., Zeiger E. (2006) *Plant Physiology*, Fourth Edition, Sinauer Associates INC Publishers, Sunderland, Massachusetts

- Takabayashi A., Kishine M., Asada K., Endo T. and Sato F. (2005) Differential use of two cyclic electron flows around photosystem I for driving CO_2-concentration mechanism in C_4 photosynthesis. *PNAS-USA* 102: 16898-16903

- Thomas D.J., Thomas J., Youderian P.A. and Herbert S.K. (2001) Photoinhibition and light-induced cyclic electron transport in ndhB(-) and psaE(-) mutants of *Synechocystis* sp. PCC 6803. *Plant Cell Physiol* 42: 803-12

- Towbin H., Staehelin T. and Gordon J. (1979) Electrophoretic transfer of proteins from polyacrylamide gels to nitrocellulose sheets: procedure and some applications. *PNAS-USA* 76: 4350-4354

- Varotto C., Pesaresi P., Maiwald D., Kurth J., S., Salamini F. and Leister D. (2000b) Identification of photosynthetic mutants of *Arabibidopsis* by automatic screening for altered effective quantum yield of photosystem II. *Photosynthetica* 38: 497-504

- Varotto C., Pesaresi P., Meurer J., Oelmuller R., Steiner-Lange S., Salamini F. and Leister D. (2000) Disruption of the *Arabidopsis* photosystem I gene *PSA-E1* affects photosynthesis and impairs growth. *Plant J* 22: 115-124

- Waegemann K. and Soll J. (1991) Characterization of the import apparatus in isolated outer envelopes of chloroplasts. *Plant J* 1: 149-159

- Wolk C.P., Ernst A. and Elhai J. (1994) Heterocyst metabolism and development. *The Molecular Biology of Cyanobacteria* ed. DA Bryant: 769-823

- Yeremenko N., Jeanjean R., Prommeenate P., Krasikov V., Nixon P.J., Vermaas W.F., Havaux M. and Matthijs H.C. (2005) Open reading frame ssr2016 is required for antimycin A-sensitive photosystem I-driven cyclic electron flow in the cyanobacterium *Synechocystis* sp. PCC 6803. *Plant Cell Physiol* 46: 1433-1436

- Yu L., Zhao J., Mühlenhoff U., Bryant D. and Golbeck J.H. (1993) PsaE is required for in vivo cyclic electron flow around photosystem I in the cyanobacterium *Synechococcus* sp. PCC 7002. *Plant Physiol* 103: 171-180

- Zhang H.M., Whitelegge J.P. and Cramer W.A. (2001) Ferredoxin:NADP$^+$ ossidoreductase is a subunit of the chloroplast cytochrome b6f complex. *J Biol Chem* 276: 38159-38165

- Zhao J., Snyder W.B., Mühlenhoff U., Rhiel E., Warren P.V., Golbeck J.H. and Bryant D.A. (1993) Cloning and characterization of the psaE gene of the cyanobacterium *Synechococcus* sp. PCC 7002: Characterization of a *psaE* mutant and overproduction of the protein in *Escherichia coli*. *Mol Microbiol* 9: 183-194

Acknowledgments

I would like to thank my supervisor, Prof. Dr. Dario Leister, who gave me the possibility to develop my way to do science during all these years of PhD, discussing about my projects and supporting me.

I thank everybody who contributed with experiments and discussions to this project: Dr. Elena Aseeva for the *in vitro* import; Prof. Dr. Peter Jahns for the pigment analysis; PD Dr. Danja Schünemann for the split ubiquitin assay; Dr. Simona Masiero for the yeast two hybrid assay; Prof. Dr. Roberto Barbato and Dr. Paolo Pesaresi for the helpful discussion and the contribution to the antibodies biosynthesis and Alexander Hertle for the PPP7A protein expression and purification. Last but not least, I thank Prof. Dr. Pierre Joliot and Dr. Giovanni Finazzi for their willingness in measuring *in vivo* cyclic electron flow.

A special thank to Prof. Dr. Toshiharu Shikanai and PD Dr. Jörg Meurer for discussion and helpful suggestions for the interpretation of my results.

Many thanks to my lab colleagues, who taught me how to cope with a different culture and how to stay in a foreign country. Special thanks to those who helped me to write this thesis reading it and giving me advices.

I am glad and thankful to have met friends, which, with their presence and sustain, supported me and stood my behaviour, making the time here lighter.

Finally, I am grateful to my family and to Maria Teresa, who have always been there for me, encouraging and helping me whenever I needed it.

É stato bello!

Curriculum vitae

PERSONAL DATA

Date of birth: 12 October 1979
Place of birth: Verona, Italy
Citizenship: Italian

RESEARCH EXPERIENCES

October 2005 – December 2007
Ludwig-Maximillians-Universität München (Germany)
Department Biology I, Botanic
- PhD continuation. Supervisor Prof. Dr. Dario Leister

July 2004 – September 2005
Max Planck Institut für Züchtungsforschung (Köln, Germany)
- PhD in "Characterization of the novel photosynthetic protein PPP7 involved in Cyclic Electron Flow around PSI". Supervisor Prof. Dr. Dario Leister

Summer 2004
Universitá degli Studi di Verona (Italy)
Dipartimento Scientifico e Tecnologico
- Technical assistant

2003 – 2004
Universitá degli Studi di Verona (Italy)
Dipartimento Scientifico e Tecnologico
- Diploma thesis in "Characterization of a bZIP transcriptional factor induced by Cadmium in *Brassica juncea* (L.) Czern". Supervisor Prof. Dr. Antonella Furini

EDUCATION

1998 – 2004
Universitá degli Studi di Verona, Italy
- Degree in Plant and Microbial Biotechnology (graduated *summa cum laude*)

1993 – 1998

Liceo Scientifico Tecnologico, Galileo Galilei, Verona, Italy

- Diploma, high school

PUBLICATIONS

- Dal Corso G., Pesaresi P., Masiero S., Aseeva E., Schünemann D., Finazzi G., Joliot P., Barbato R. and Leister D. (2008) A complex of PGRL1 and PGR5 is involved in the switch between linear and ferredoxin-dependent cyclic electron flow. *Cell*: accepted

- Noutsos C., Kleine T., Armbruster U., Dal Corso G. and Leister D. (2007) Nuclear insertions of organellar DNA can create novel patches of functional exon sequences. *Trends Genet* Nov 2; (Epub ahead of print)

- Dal Corso G., Borgato L. and Furini A. (2005) In vitro plant regeneration of the heavy metal tolerant and hyperaccumulator *Arabidopsis halleri* (*Brassicaceae*). *Plant Cell, Tissue and Organ Culture* 82: 267-270

- Fusco N., Micheletto L., Dal Corso G., Borgato L. and Furini A. (2005) Identification of Cadmium-regulated genes by cDNA-AFLP in the heavy metal accumulator *Brassica juncea. Journal of Experimental Botany* 56: 3017-3027

POSTERS

- Fusco N., Dal Corso G., Borgato L, Furini A: Transcription profile of genes induced by cadmium in *Brassica juncea* for phytoremediation. SIGA meeting Verona (Italy), 24-27 September 2003

- Furini A., Fusco N., Dal Corso G., Micheletto L. and Borgato L.: Transcription profile of genes induced by cadmium in *Brassica juncea*. Phytoremediation: OECD Environmental and Molecular Biological Aspects. Mátraháza (Hungary), 9-12 September 2004

LANGUAGES

- Italian, mother tongue
- English, fluent
- German, basic

Ehrenwörtliche Versicherung

Hiermit versichere ich, dass ich die vorliegende Arbeit selbständig und nur unter Verwendung der angegebenen Hilfsmittel und Quellen angefertigt habe. Der Autor hat zuvor nicht versucht, anderweitig eine Dissertation einzureichen oder sich einer Doktorprüfung zu unterziehen. Die Dissertation wurde keiner weiteren Prüfungskommission weder in Teilen noch als Ganzes vorgelegt.

München,
Dezember 2007

Giovanni Dal Corso